Toxicology and Applied Pharmacology 272 (2013) 154–160

Contents lists available at ScienceDirect

Toxicology and Applied Pharmacology

journal homepage: www.elsevier.com/locate/ytaap

Cigarette smoking substantially alters plasma microRNA profiles in healthy subjects

Kei Takahashi [1], Shin-ichi Yokota [1], Naoyuki Tatsumi, Tatsuki Fukami, Tsuyoshi Yokoi, Miki Nakajima *

Drug Metabolism and Toxicology, Faculty of Pharmaceutical Sciences, Kanazawa University, Kakuma-machi, Kanazawa 920-1192, Japan

ARTICLE INFO

Article history:
Received 16 March 2013
Revised 16 May 2013
Accepted 18 May 2013
Available online 29 May 2013

Keywords:
MicroRNA
Smoking
Biomarker

ABSTRACT

Circulating microRNAs (miRNAs) are receiving attention as potential biomarkers of various diseases, including cancers, chronic obstructive pulmonary disease, and cardiovascular disease. However, it is unknown whether the levels of circulating miRNAs in a healthy subject might vary with external factors in daily life. In this study, we investigated whether cigarette smoking, a habit that has spread throughout the world and is a risk factor for various diseases, affects plasma miRNA profiles. We determined the profiles of 11 smokers and 7 non-smokers by TaqMan MicroRNA array analysis. A larger number of miRNAs were detected in smokers than in non-smokers, and the plasma levels of two-thirds of the detected miRNAs (43 miRNAs) were significantly higher in smokers than in non-smokers. A principal component analysis of the plasma miRNA profiles clearly separated smokers and non-smokers. Twenty-four of the miRNAs were previously reported to be potential biomarkers of disease, suggesting the possibility that smoking status might interfere with the diagnosis of disease. Interestingly, we found that quitting smoking altered the plasma miRNA profiles to resemble those of non-smokers. These results suggested that the differences in the plasma miRNA profiles between smokers and non-smokers could be attributed to cigarette smoking. In addition, we found that an acute exposure of ex-smokers to cigarette smoke (smoking one cigarette) did not cause a dramatic change in the plasma miRNA profile. In conclusion, we found that repeated cigarette smoking substantially alters the plasma miRNA profile, interfering with the diagnosis of disease or signaling potential smoking-related diseases.

Introduction

MicroRNAs (miRNAs) are a class of endogenous, short non-coding RNAs 19–25 nucleotides in length that negatively regulate gene expression via translational repression or mRNA degradation, primarily by pairing with the 3′-untranslated regions of the target mRNAs (Ambros, 2001). More than 2,000 human miRNAs have been identified (miRBase ver. 19). It is now clear that miRNAs are involved in various important biological processes, including cell differentiation, proliferation, apoptosis, and development (He and Hannon, 2004; Meltzer, 2005). Some miRNAs are expressed in a tissue-specific manner, and others are ubiquitously expressed (Liang et al., 2007). It is also known that miRNA expression is significantly altered in several diseases (http://www.miR2disease.org/), and the dysregulation of miRNAs is closely linked with the incidence or progress of these diseases.

It was reported in 2008 that miRNAs exist in plasma or serum (Mitchell et al., 2008). Subsequent reports have revealed the presence of miRNAs in saliva (Michael et al., 2010; Park et al., 2009) and urine (Hanke et al., 2010). These extracellular miRNAs are stable in the RNase-rich environment because they are enclosed in vesicles, including exosomes, microvesicles, apoptotic bodies, and ectosomes (Lee et al., 2012), or are associated with RNA-binding proteins, including nucleophosmin 1 (Wang et al., 2010b) or high-density lipoprotein (Vickers et al., 2011). Following the discovery of extracellular miRNA in body fluids, a significant number of papers reported that the levels of some extracellular miRNAs are linked to different pathophysiological conditions. Examples of this include the associations of miR-141 and miR-375 with prostate cancer (Bryant et al., 2012), miR-29a and miR-92a with colorectal cancer (Huang et al., 2010), miR-499 with myocardial infarction (Olivieri et al., in press), and miR-122 with liver injury (Wang et al., 2009). These findings introduce the possibility of using the levels of specific miRNAs in body fluids as biomarkers for different pathological conditions (Duttagupta et al., 2011; Wang et al., 2012b). However, it is unknown whether the levels of extracellular miRNAs in a healthy subject might vary with external factors in daily life.

Cigarette smoking is a habit that has spread all over the world and is a significant risk factor for many diseases, including lung cancer (Shields, 1999), chronic obstructive pulmonary disease (Higgins et al., 1984), asthma (Ulrik and Lange, 2001) and cardiovascular disease (Holbrook et al., 1984). Cigarette smoke contains over 4800 chemicals, including 69 carcinogens (Hoffmann et al., 2001), which appear to be of crucial importance in causing disease. We questioned whether cigarette smoking alters plasma miRNA

* Corresponding author. Fax: +81 76 234 4407.
E-mail address: nmiki@p.kanazawa-u.ac.jp (M. Nakajima).
[1] K.T. and S.Y. contributed equally to this work.

0041-008X/$ – see front matter © 2013 Elsevier Inc. All rights reserved.
http://dx.doi.org/10.1016/j.taap.2013.05.018

profiles in humans, and, if it does, whether the changes may be associated with the pathogenesis of various diseases. In this study, we compared the plasma miRNA profiles of smokers and non-smokers and discussed the biological significance of the different profiles by the smoking status.

Materials and methods

Chemicals and reagents. The *mir*Vana PARIS Kit, Megaplex pools, TaqMan microRNA Reverse Transcription Kit, TaqMan Universal PCR Master Mix (No AmpErase UNG) and TaqMan Human MicroRNA Array A and B Card v2.0 were from Life Technologies (Carlsbad, CA). Nicotine and cotinine were purchased from Sigma (St. Louis, MO). Acetanilide was purchased from Wako (Osaka, Japan). All other chemicals and solvents were of the highest grade commercially available.

Study design. This study was approved by the Ethics Committee of Kanazawa University (Kanazawa, Japan). Written, informed consent was obtained from all the subjects. Eleven smokers (S1–S11) and seven non-smokers (NS1–NS7) who were healthy male Japanese taking no medicines or supplements were recruited (Table 1). The smokers smoked their favorite brands of cigarettes as shown in Table 1. The pack year (number of cigarettes per day × number of years smoked/20 cigarettes in one pack) ranged from 4 to 35 (18 ± 9). There were no significant differences in the age and body weight of the smokers and non-smokers.

This study consists of three experiments. For the blood collection (5 ml), subjects came at 10 AM without having had breakfast. In experiment I, blood was collected from all subjects to compare the plasma miRNA profiles in smokers and non-smokers. Smoking occurred in the morning or not, according to each smoker's habit. After experiment I, we noticed that four smokers (S1, S2, S4, and S8) had voluntarily quit smoking. Among them, subject S8 had used nicotine patches after experiment I. In experiment II, blood was collected from the four subjects to determine their plasma miRNA profiles after they quit smoking (S1, S2, and S4 were tested one month after quitting; S8 was tested three months after quitting but was using nicotine patches). After that, two subjects, S1 and S4, returned to smoking. We had asked them to contact us when they began smoking again. In experiment III, blood was collected from the two subjects (S1 and S4) 20 min after they smoked the first cigarette (Mild Seven, Japan Tobacco, Tokyo, Japan) to determine the plasma miRNA profiles immediately after exposure to cigarette smoke.

RNA isolation from plasma. Ethylenediamine-*N,N,N′,N′*-tetraacetic acid disodium salt was added as an anticoagulant to the blood, which was then kept at room temperature for 30 min. After centrifugation at 3000 g for 10 min at 4 °C, the plasma was collected. Immediately, total RNA was isolated from 600 μl of plasma using the *mir*Vana PARIS kit as described previously (Yamaura et al., 2012).

Taqman microRNA array analysis. The expression profiles of miRNAs were assessed using TaqMan Human MicroRNA Array A + B Cards Sets v2.0 containing 377 (A array) or 287 (B array) primer-probe sets for individual miRNAs (total 664 miRNAs). All procedures were performed following the manufacturer's instructions. Briefly, 3 μl of total RNA was reverse transcribed using Megaplex RT Primer Pool A or B and TaqMan MicroRNA Reverse Transcription Kits. Pre-amplification was carried out using Megaplex PreAmp primers and the TaqMan Pre-amp Master Mix. The expression of miRNAs was determined by quantitative real-time PCR using the TaqMan Human MicroRNA Array with the 7900HT Fast Real-Time PCR System (Life Technologies) and the manufacturer's recommended cycling conditions. Cycle threshold (Ct) values were calculated using the SDS software v.2.3 with a baseline of 3-15 and an assigned minimum threshold of 0.2. Expression of miRNAs was normalized by global normalization, which implicitly assumes that the mean expression level of all monitored miRNAs is constant. Any miRNA giving 40-Ct < 8, a cutoff value recommended by the manufacturer, in at least one sample was omitted from the data analysis.

Principal component analysis. The plasma miRNA expression data were analyzed using the Partek Genomics Suite version 6.12 (Partek, St. Louis, MO). Principal component analysis (PCA) was performed to visualize the difference between groups of the expression profiles of miRNAs that exceeded the cutoff value.

Measurement of plasma concentrations of nicotine and cotinine. Plasma concentrations of nicotine and cotinine were measured as described previously (Nakajima et al., 2000) with slight modifications. The plasma sample (0.5 ml) was alkalinized with 25 μl of 10 M NaOH. After the addition of 10 μl of 7 μM acetanilide as an internal standard, the mixture was extracted with 4 ml dichloromethane by shaking for 10 min.

Table 1
Characteristics of subjects.

Subject	Age (years)	Height (cm)	Body weight (kg)	Brand of cigarette	Nicotine (mg)	Tar (mg)	Age at starting smoking (years)	Number of cigarettes per day	Number of years smoked (years)	Pack-year
S1	36	168	50	Mild Seven	0.7	8	20	15	16	12
S2	41	170	64	Mild Seven Lights	0.7	8	20	20	21	21
S3	35	169	65	Mild Seven	0.8	10	20	30	15	23
S4	55	177	68	Marlboro	1.0	12	20	20	35	35
S5	21	172	80	Hi-Lite Menthol	0.7	10	16	15	5	4
S6	46	165	53	Hi-Lite	1.4	17	20	20	26	26
S7	38	167	57	Mild Seven Aqua Menthol	0.1	1	20	10	18	9
S8	37	165	58	Lark Menthol	0.1	1	20	20	17	17
S9	40	156	53	Cabin	0.4	5	18	20	22	22
S10	36	172	55	Mild Seven Super Lights	0.5	6	20	20	16	16
S11	39	168	65	Kool Mild	0.7	8	16	10	23	12
Mean ± SD	38.5 ± 8.2	168 ± 5.0	61.7 ± 8.7		0.6 ± 0.4	8 ± 5		18 ± 6	19 ± 8	18 ± 9
NS1	26	163	65							
NS2	39	177	84							
NS3	50	164	63							
NS4	29	169	62							
NS5	41	173	80							
NS6	43	161	57							
NS7	28	170	67							
Mean ± SD	36.6 ± 9.0	168.1 ± 5.8	68.3 ± 9.9							

After centrifugation at 1000 g for 10 min, 12 μl of 12 M HCl was added to the organic fraction. The organic fraction was evaporated with a vacuum evaporator at 40 °C. The residue was redissolved in 50 μl of the mobile phase, and then a 20 μl portion of the sample was subjected to liquid chromatography/tandem mass spectrometry (LC-MS/MS). The LC-MS/MS condition was described in our previous report (Yamanaka et al., 2004).

Statistical analysis. Data are presented as the mean ± standard deviation. Statistical analyses of the differences between two groups were performed by an unpaired two-tailed Student's *t*-test. A value of *P* less than 0.05 was considered statistically significant.

Results

Plasma miRNA profiles of non-smokers and smokers

We determined plasma miRNA expression in 11 smokers and 7 non-smokers by quantitative real-time PCR using the TaqMan MicroRNA Array. The numbers of miRNAs with 40-Ct > 8 in each individual are shown in Table 2. The numbers in smokers (196 ± 18) were significantly ($P < 0.001$) larger than those in non-smokers (143 ± 29). The number of miRNAs that exceeded the cutoff value in all subjects (n = 18) was 66. We compared the levels of 66 miRNAs in smokers and non-smokers. Among them, 44 miRNAs showed a significant difference between the groups (Table 3). Forty-three miRNAs were higher in smokers than in non-smokers, whereas 1 miRNA was lower in smokers than in non-smokers. To visualize the difference in the expression profiles of miRNAs between smokers and non-smokers, PCA was performed using the expression data for the 66 miRNAs. PC1 encompassed a significantly large proportion (63%) of the total variance for each subject, followed by PC2 (10%) and PC3 (6%). As shown in Fig. 1, the profiles of plasma miRNA expression of the smokers were different from those of the non-smokers.

Quitting smoking altered the plasma miRNA profile

To investigate whether the difference in the plasma miRNA profiles between smokers and non-smokers was due to cigarette smoking, we examined miRNA expression in the plasma of 4 smokers who had stopped smoking (S1, S2, S4, and S8). To confirm their non-smoking status, we measured their plasma concentrations of nicotine and cotinine. For comparison, nicotine and cotinine concentrations were also measured when they were still smoking (experiment I); these concentrations were 3.6–26.0 ng/ml and 23.4–413.0 ng/ml, respectively (Table 4). One month after they stopped smoking, the levels in S1 and S2 had dramatically decreased to values close to the detection limit. In the plasma from S4, low levels of nicotine and cotinine were detected; therefore, he might have been smoking in secret or been exposed to

Table 3
Forty-four plasma miRNAs are differently ($P < 0.05$) expressed in 7 non-smokers (NS) compared to 11 smokers (S).

microRNA	40 - Ct value (Mean ± SD)		Fold (S/NS)	*P*-value
	NS	S		
miR-374b	12.75 ± 2.89	15.76 ± 1.03	8.11	0.006
miR-331-3p	11.72 ± 2.85	14.61 ± 1.26	7.39	0.009
miR-221	12.84 ± 2.46	15.61 ± 1.57	6.83	0.010
let-7g	12.85 ± 1.78	15.40 ± 0.89	5.89	0.001
miR-301a	10.66 ± 1.79	13.09 ± 0.78	5.39	0.001
let-7e	15.47 ± 1.07	17.74 ± 1.13	4.83	0.001
miR-335	11.21 ± 1.94	13.48 ± 0.80	4.83	0.003
miR-26a	14.91 ± 1.45	17.09 ± 0.91	4.51	0.001
miR-30c	15.21 ± 1.13	17.35 ± 0.82	4.40	0.000
miR-185	10.65 ± 2.06	12.77 ± 0.67	4.36	0.005
miR-374a	13.71 ± 1.50	15.83 ± 0.96	4.36	0.002
miR-30b	15.24 ± 1.20	17.36 ± 0.76	4.33	0.000
let-7b	14.33 ± 1.06	16.43 ± 0.94	4.30	0.000
miR-451	15.62 ± 1.75	17.70 ± 1.61	4.22	0.020
miR-27a	12.36 ± 2.02	14.26 ± 0.48	3.74	0.008
miR-29a	12.78 ± 1.32	14.64 ± 0.43	3.63	0.000
miR-191	18.18 ± 1.79	20.04 ± 0.87	3.63	0.009
miR-26b	14.15 ± 1.33	15.99 ± 0.75	3.59	0.002
miR-199a-3p	14.49 ± 1.54	16.30 ± 0.82	3.52	0.005
miR-425	12.11 ± 1.50	13.92 ± 0.78	3.51	0.004
miR-223	21.95 ± 1.59	23.70 ± 0.45	3.36	0.003
miR-328	13.18 ± 1.91	14.87 ± 0.94	3.23	0.023
miR-21	14.41 ± 1.42	16.06 ± 0.38	3.14	0.002
let-7d	13.32 ± 0.94	14.97 ± 0.91	3.12	0.002
miR-19b	18.36 ± 1.39	20.00 ± 0.56	3.12	0.003
miR-106b	13.34 ± 1.71	14.92 ± 0.82	2.99	0.017
miR-19a	14.53 ± 1.29	16.10 ± 0.53	2.96	0.002
miR-186	15.79 ± 1.55	17.33 ± 0.60	2.92	0.008
miR-93	14.99 ± 1.67	16.44 ± 0.73	2.72	0.021
miR-454	14.12 ± 1.00	15.52 ± 0.88	2.64	0.007
miR-345	11.46 ± 1.29	12.86 ± 0.71	2.63	0.009
miR-20b	15.24 ± 1.44	16.60 ± 0.36	2.57	0.008
miR-17	18.67 ± 1.31	19.89 ± 0.50	2.33	0.013
miR-20a	18.08 ± 1.31	19.29 ± 0.58	2.32	0.015
miR-24	18.26 ± 1.58	19.43 ± 0.74	2.25	0.048
miR-106a	18.58 ± 1.43	19.75 ± 0.56	2.25	0.026
miR-126	19.24 ± 1.06	20.41 ± 0.75	2.24	0.015
miR-16	20.12 ± 1.09	21.26 ± 0.78	2.19	0.020
miR-25	13.92 ± 1.18	15.04 ± 0.68	2.18	0.020
miR-923	13.19 ± 1.59	14.31 ± 0.58	2.16	0.016
miR-195	14.69 ± 1.10	15.79 ± 0.91	2.14	0.035
miR-126*	16.28 ± 1.02	17.33 ± 0.58	2.07	0.013
miR-92a	17.36 ± 0.81	18.12 ± 0.64	1.70	0.039
miR-188-5p	12.90 ± 0.95	12.05 ± 0.74	0.55	0.047

Plasma miRNAs shaded with gray have been reported to be candidate biomarkers of diseases (Table 6).

Table 2
The numbers of plasma miRNAs with 40-Ct > 8 in non-smokers (NS) and smokers (S).

Non-smokers		Smokers		Status		
				Smoking	Quit	Acute exposure
NS1	174	S1	198	198	160	177
NS2	191	S2	216	216	138	
NS3	138	S3	208			
NS4	138	S4	234	234	129	131
NS5	110	S5	189			
NS6	121	S6	189			
NS7	129	S7	185			
		S8	187	187	137	
		S9	177			
		S10	170			
		S11	200			
Mean ± SD	143 ± 29	Mean ± SD	196 ± 18***	209 ± 21	141 ± 13##	

*** $P < 0.001$, compared with non-smokers.
$P < 0.01$, compared with smoking status in 4 smokers (S1, S2, S4, and S8).

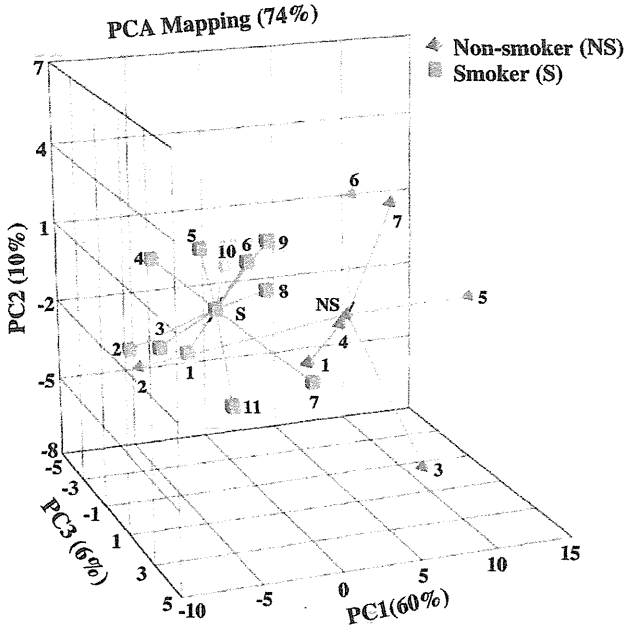

Fig. 1. PCA of plasma miRNA expression in 7 non-smokers (NS) and 11 smokers (S). PCA was performed using 66 miRNAs that exceeded the cutoff value in all subjects (n = 18). A three-component model was developed that explained a total of 79% (PC1, 63%; PC2, 10%; PC3, 6%) of the variability of the data. Each ball representing an individual is connected to the centroid (marked as NS or S) of each group. The numbers near the balls represent the subject number. This plot illustrates the level of spread between individuals and groups using three principal components.

passive smoking. S8 showed substantial nicotine and cotinine levels comparable to those of active smokers. These levels were not surprising because this subject used nicotine patches.

The numbers of miRNAs with 40-Ct > 8 in the 4 subjects who had stopped smoking were 141 ± 13 (129–160). Interestingly, the number was very close to that in non-smokers (143 ± 29) and was significantly ($P < 0.01$) lower than that when they were still smoking (209 ± 21) (Table 2). We compared the plasma miRNA expression in the four subjects before and after they stopped smoking. The numbers of miRNAs that exceeded the cutoff value in the four subjects was 93. Among them, 63 miRNAs showed a significant difference between the groups (Table 5). Sixty miRNAs were significantly lower after the subjects had stopped smoking than before they stopped, whereas 3 miRNAs were significantly higher after they stopped than before they stopped. Interestingly, among the 60 miRNAs that were lower after the subjects had stopped smoking, 38 miRNAs (shaded in Table 5) were the ones more highly expressed in smokers than in non-smokers (Table 2). These results suggested that the plasma miRNA expression is unambiguously affected by smoking.

We considered the possibility that quitting smoking might alter the plasma miRNA profiles to resemble the profiles of non-smokers. To test this possibility, we compared the plasma miRNA profiles of the 4 subjects before and after they stopped smoking, as well as the profiles of the 7 non-smokers. The number of miRNAs exceeding the cutoff value among the three groups was 66. PCA was performed using the expression data of the 66 miRNAs (Fig. 2A). PC1 encompassed the largest

Table 4
Plasma concentrations of nicotine and cotinine in 4 smokers who quit smoking for at least one month and then smoked again.

Smoker	Nicotine (ng/ml)			Cotinine (ng/ml)		
	Status			Status		
	Smoking	Quit	Acute exposure	Smoking	Quit	Acute exposure
S1	3.6	0.1	13.7	282.1	1.1	5.1
S2	16.3	1.0		23.4	0.6	
S4	16.7	3.3	15.7	413.0	9.5	17.9
S8	26.0	25.9		243.5	364.3	

Table 5
Sixty-three plasma miRNAs differently ($P < 0.05$) expressed in 4 subjects (S1, S2, S4, and S8) who smoked (S) and then quit smoking (Q).

microRNA	40-Ct values (Mean ± SD)		Fold (Q/S)	P-value
	S	Q		
hsa-miR-766	15.07 ± 1.48	10.44 ± 0.92	0.04	0.002
hsa-miR-374b	16.30 ± 0.47	11.73 ± 0.87	0.04	0.000
hsa-miR-340	13.41 ± 0.32	9.64 ± 1.05	0.07	0.000
hsa-let-7e	18.30 ± 1.06	14.57 ± 0.50	0.08	0.001
hsa-miR-191	20.53 ± 0.80	16.85 ± 0.65	0.08	0.000
hsa-miR-103	13.99 ± 1.22	10.34 ± 1.98	0.08	0.020
hsa-miR-199a-3p	16.67 ± 0.91	13.13 ± 0.46	0.09	0.000
hsa-miR-625*	14.33 ± 1.50	10.83 ± 0.53	0.09	0.005
hsa-miR-186	17.45 ± 0.47	14.01 ± 0.96	0.09	0.001
hsa-let-7g	15.68 ± 0.86	12.25 ± 1.41	0.09	0.006
hsa-miR-185	12.85 ± 0.54	9.43 ± 0.84	0.09	0.000
hsa-miR-197	15.88 ± 0.97	12.52 ± 1.36	0.10	0.007
hsa-miR-331-3p	15.43 ± 0.91	12.19 ± 0.76	0.11	0.002
hsa-miR-454	15.71 ± 0.91	12.50 ± 0.33	0.11	0.001
hsa-miR-374a	16.15 ± 0.49	12.95 ± 0.84	0.11	0.001
hsa-let-7b	16.62 ± 1.04	13.52 ± 0.70	0.12	0.003
hsa-miR-495	12.63 ± 0.42	9.54 ± 0.76	0.12	0.000
hsa-let-7d	15.36 ± 0.78	12.44 ± 0.70	0.13	0.001
hsa-miR-484	19.64 ± 0.80	16.77 ± 0.94	0.14	0.004
hsa-miR-19a	16.28 ± 0.18	13.51 ± 0.99	0.15	0.001
hsa-miR-301a	13.38 ± 0.62	10.65 ± 0.76	0.15	0.001
hsa-miR-26a	17.63 ± 0.70	14.93 ± 0.95	0.15	0.004
hsa-miR-151-3p	15.05 ± 1.23	12.35 ± 0.30	0.15	0.005
hsa-miR-335	13.88 ± 0.77	11.21 ± 0.54	0.16	0.001
hsa-miR-181a	17.87 ± 1.20	9.21 ± 0.84	0.16	0.011
hsa-miR-222	19.08 ± 0.74	16.44 ± 1.15	0.16	0.008
hsa-miR-28-3p	14.60 ± 0.79	11.98 ± 1.10	0.16	0.008
hsa-miR-590-5p	14.43 ± 0.24	11.82 ± 0.26	0.16	0.000
hsa-miR-140-5p	15.85 ± 0.76	13.28 ± 0.67	0.17	0.002
hsa-miR-30b	17.77 ± 0.51	15.20 ± 0.83	0.17	0.002
hsa-miR-30d	12.03 ± 1.26	9.47 ± 0.98	0.17	0.018
hsa-miR-15b	15.56 ± 0.58	13.03 ± 0.78	0.17	0.002
hsa-miR-20b	16.63 ± 0.30	14.14 ± 0.82	0.18	0.001
hsa-miR-93	16.81 ± 0.69	14.38 ± 0.92	0.19	0.006
hsa-miR-223	23.87 ± 0.27	21.45 ± 0.45	0.19	0.000
hsa-miR-342-3p	17.36 ± 0.42	15.00 ± 0.10	0.19	0.007
hsa-miR-320	18.79 ± 0.88	16.45 ± 0.71	0.20	0.006
hsa-miR-28-5p	12.55 ± 0.73	10.23 ± 1.06	0.20	0.011
hsa-miR-328	15.56 ± 0.91	13.25 ± 0.08	0.20	0.002
hsa-miR-24	19.90 ± 0.65	17.63 ± 0.52	0.21	0.002
hsa-miR-126	20.70 ± 0.57	18.57 ± 0.49	0.23	0.001
hsa-miR-26b	16.19 ± 0.33	14.07 ± 0.80	0.23	0.003
hsa-miR-152	12.97 ± 0.65	10.89 ± 0.19	0.24	0.022
hsa-miR-27a	14.50 ± 0.37	12.51 ± 0.29	0.25	0.000
hsa-miR-17	20.04 ± 0.45	18.05 ± 0.65	0.25	0.002
hsa-miR-30c	17.78 ± 0.66	15.82 ± 0.90	0.26	0.013
hsa-miR-19b	20.02 ± 0.28	18.21 ± 0.72	0.28	0.003
hsa-miR-106a	19.90 ± 0.63	18.09 ± 0.39	0.29	0.003
hsa-miR-20a	19.41 ± 0.36	17.61 ± 0.48	0.29	0.001
hsa-miR-923	14.40 ± 0.85	12.66 ± 0.88	0.30	0.030
hsa-miR-29a	14.62 ± 0.48	12.93 ± 0.33	0.31	0.001
hsa-miR-345	13.14 ± 0.88	11.46 ± 0.61	0.31	0.020
hsa-miR-18a	13.32 ± 0.53	11.64 ± 0.23	0.31	0.001
hsa-miR-106b	14.88 ± 0.22	16.42 ± 0.43	0.36	0.001
hsa-miR-16	21.06 ± 0.45	19.60 ± 0.65	0.36	0.010
hsa-miR-126*	17.04 ± 0.35	15.60 ± 0.95	0.37	0.029
hsa-miR-532-5p	12.25 ± 0.76	10.83 ± 0.53	0.37	0.022
hsa-miR-148a	12.15 ± 0.66	10.90 ± 0.78	0.42	0.050
hsa-miR-92a	18.31 ± 0.42	17.07 ± 0.65	0.42	0.019
hsa-miR-21	15.98 ± 0.36	14.81 ± 0.65	0.45	0.020
hsa-miR-135a*	15.80 ± 0.88	17.06 ± 0.39	2.39	0.039
hsa-miR-188-5p	11.68 ± 0.45	13.20 ± 0.12	2.86	0.001
hsa-miR-138-1*	11.61 ± 1.31	14.36 ± 0.21	6.73	0.006

Plasma miRNAs shaded with gray were more highly expressed in smokers than in non-smokers (Table 3).

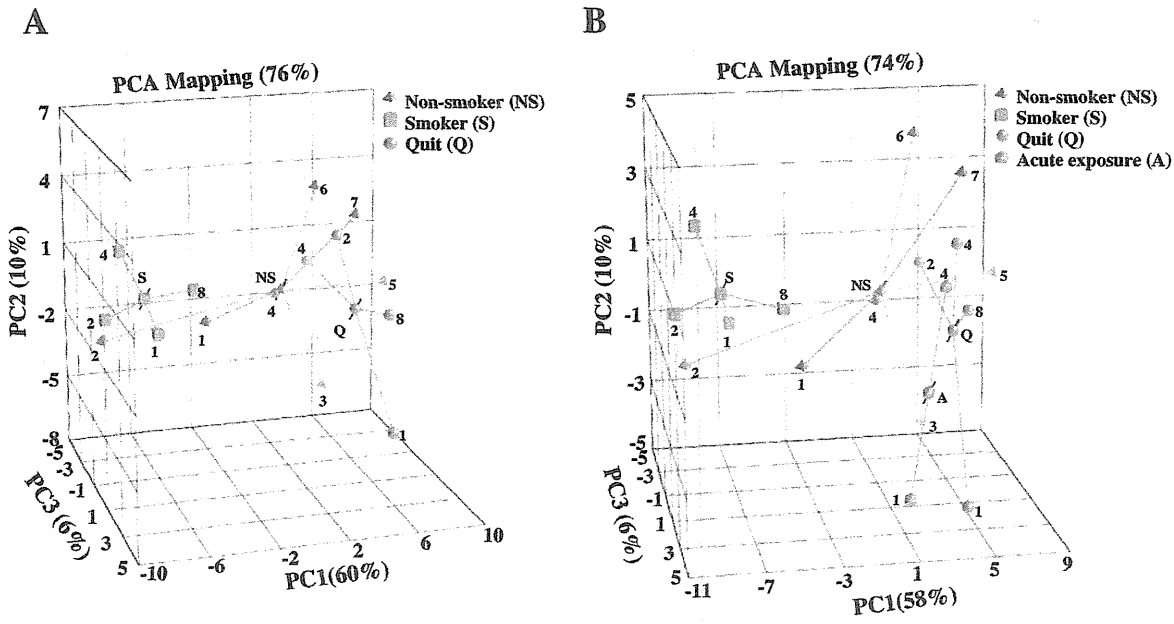

Fig. 2. The effects of quitting smoking and of subsequently smoking one cigarette on plasma miRNA profiles. (A) PCA was performed using 66 miRNAs that exceeded the cutoff value in 4 subjects who smoked and who quit smoking, as well as in 7 non-smokers. A three-component model was developed explaining a total of 76% (PC1, 60%; PC2, 10%; PC3, 6%) of the variability of the data. Each ball representing an individual is connected to the centroid (marked as NS, S, or Q) of each group. The numbers near the balls represent the subject number. (B) PCA for the expression of 66 miRNAs in 4 groups: 4 subjects who smoked and who quit smoking, 7 non-smokers and 2 subjects who quit smoking but then smoked one cigarette. A three-component model was developed explaining a total of 74% (PC1, 58%; PC2, 10%; PC3, 6%) of the variability of the data. Each ball representing an individual is connected to the centroid (marked as NS, S, Q, or A) of each group.

proportion (60%) of the total variance for each subject, followed by PC2 (10%) and PC3 (6%). These results clearly demonstrated that the plasma miRNA profiles of smokers were altered after they stopped smoking, and the profiles then resembled those of non-smokers.

Smoking one cigarette does not cause a dramatic change in the expression of plasma miRNAs

To ascertain how quickly the plasma miRNA profile was changed by smoking, we examined plasma miRNA profiles 20 min after 2 ex-smokers (S1 and S4) had each smoked one cigarette. We chose this time because it is near the Cmax values of nicotine and cotinine after smoking (Yamanaka et al., 2004). The plasma concentrations of nicotine after one cigarette were 13.7 ng/ml and 15.7 ng/ml, and those of cotinine were 5.1 ng/ml and 17.9 ng/ml (Table 4), suggesting that the subjects had inhaled the cigarette smoke. The numbers of miRNAs with 40-Ct > 8 were 177 and 131, slightly larger than the numbers of miRNAs prior to smoking the cigarettes (Table 2). The miRNA expression data were included in the PCA for the 66 miRNAs described above. As shown in Fig. 2B, the miRNA profiles after smoking one cigarette were similar to those of the smokers who had stopped smoking and the non-smokers. These results suggest that changes in the plasma miRNA profiles in smokers might be due to repeated smoking.

Discussion

Circulating miRNAs have received considerable attention as potential biomarkers of various diseases (Reid et al., 2011) based on many studies reporting differences in plasma or serum miRNA levels between healthy subjects and patients. However, it remains unclear to what extent the circulating miRNA profiles in healthy subjects vary in daily life due to changes in diet, supplements, alcohol intake, cigarette smoking, exposure to environmental chemicals, sleeping or circadian rhythm, stress, and exercise or other factors. In the present study, we focused on cigarette smoking because it is a habit spread all over the world and is a significant risk factor for various diseases including cancer. In the present investigation of the plasma miRNA profiles of smokers and non-smokers, the subjects were limited to men because a study had reported subtle sex differences (Ji et al., 2009), although another study reported no large sex differences in plasma miRNA expression (Chen et al., 2008), and because smoking is more prevalent in men than in women in Japan. In addition, considering the potential effects of circadian rhythm (Shende et al., 2011), we standardized the time of blood collection.

We found that a larger number of miRNAs were detected in smokers than in non-smokers, and the plasma levels of two-thirds of the detected miRNAs (43 miRNAs) were significantly higher in smokers than in non-smokers (Table 3). Interestingly, we found that quitting smoking changed the plasma miRNA profiles resembling those of the non-smokers (Fig. 2A). These results suggested that the differences in the plasma miRNA profiles of smokers and non-smokers were actually due to cigarette smoking. However, no association was observed between the numbers of detected miRNAs or abundance of miRNAs and plasma nicotine or cotinine levels or smoking history within smokers (data not shown). One subject who stopped smoking, S8, was a nicotine patch user. Because there was no substantial difference between the plasma miRNA profile of this subject and those of the other 3 subjects who stopped smoking, as well as those of the non-smokers, nicotine is unlikely to cause altered plasma miRNA expression. Other chemicals or oxidants in cigarette smoke, or hypoxic stress, might cause changes in plasma miRNA profiles. It would be of interest to investigate whether the miRNAs whose levels were higher in smokers than in non-smokers might be positively correlated with plasma levels of oxidative stress markers such as 8-hydroxydeoxyguanosine or malondialdehyde in smokers. It has been reported that the plasma levels of these markers were approximately 1.5 times higher in smoker than in non-smokers (Bloomer, 2007; Yamaguchi et al., 2005). Interestingly, Yamaguchi et al. (2005) reported that the levels of these oxidative stress markers were further increased within 30 min by smoking one cigarette after quitting smoking at least 10 h. The results were in contrast to our finding for miRNAs that the exposure to smoke from one cigarette did not substantially change the plasma miRNA profile. In addition, our finding is

inconsistent with a previous study reporting that urinary genotoxicity was detected 2 h after smoking one cigarette (De Flora et al., 1996). Although miR-210 and miR-373 are known to be typical miRNAs whose expression in cells was changed in response to hypoxia (Crosby et al., 2009), the levels of these miRNAs in plasma were below the cutoff values in both of smokers and non-smokers in our study. Collectively, there might be a time lag between the changes of intracellular miRNA expression and those of extracellular miRNA levels. Alternatively, consecutive and/or dynamic change of intracellular miRNA expression might be required to be reflected to the change of extracellular miRNA levels. We claim that the differences in the plasma miRNA profiles between smokers and non-smokers could be attributed to repeated smoking. An understanding of the number of cigarettes or the frequency of smoking required to cause changes in plasma miRNA profiles is left for future studies.

It is generally accepted that extracellular miRNAs mirror changes in miRNA expression in cells or tissues (Lee et al., 2012). There are some reports of the effects of cigarette smoke on miRNA expression in tissues (De Flora et al., 2012). Exposure to cigarette smoke caused down-regulation of some miRNAs in mouse and rat lungs (Izzotti et al., 2009a, 2009b), and the down-regulation in mouse lung was reversed by smoking cessation (Izzotti et al., 2011). Similar findings have been reported in humans; the levels of several miRNAs in airway epithelium (Schembri et al., 2009), placenta (Maccani et al., 2010), and alveolar macrophages (Graff et al., 2012) were lower in smokers than in non-smokers. These results led us to speculate that miRNAs in tissues, including trachea and lung, exposed to cigarette smoke might leak into blood. This might be the reason for higher levels of circulating miRNAs in smokers. Although it is not known whether extracellular miRNAs are functional, miRNAs undoubtedly function in cells; therefore, changes in miRNA expression in tissues or cells caused by exposure to cigarette smoke may have some pathophysiological significance. Integrated analysis of the expression of circulating miRNAs and the dysregulation of miRNAs and their target genes in tissues could provide insight into the initiation and progression of smoking-related diseases.

Interestingly, we noticed that 24 of the 44 miRNAs that showed a significantly different expression between smokers and non-smokers were previously reported as potential biomarkers of diseases (Table 6). Our observations show that smoking status might lead to incorrect conclusions when circulating miRNAs are used as biomarkers of diseases. Smoking status should therefore be considered when using circulating miRNAs as biomarkers of disease.

In conclusion, we found that cigarette smoking unambiguously alters plasma miRNA profiles. A larger number of miRNAs were detected and their expression levels were higher in smokers than in non-smokers. Because more than half of the miRNAs were reported to be potential biomarkers of diseases, we suggest the possibility that smoking status might complicate diagnosis. The plasma miRNA profiles that mirror changes in miRNA expression in tissues might signal smoking-related diseases. The information presented here provides new insight into an area of future research on circulating miRNAs.

Table 6
Circulating miRNAs reported to be potential biomarkers of diseases in humans.

miRNA	Disease
hsa-miR-221	Colorectal cancer↑ (Pu et al., 2010), malignant melanoma↑ (Kanemaru et al., 2011)
let-7 g	Breast cancer↑(Cookson et al., 2012)
hsa-let-7e	Papillary thyroid carcinomas↑(Yu et al., 2012)
hsa-miR-26a	Pancreatic cancer↑(Mahn et al., 2011), Type 1 diabetes↑(Nielsen et al., 2012)
hsa-miR-30c	Acute myocardial infarction↑(Meder et al., 2011)
hsa-let-7b	Acute myocardial infarction↑(Long et al., 2012b)
hsa-miR-451	Systemic lupus erythematosus↑(Wang et al., 2012a), renal cell carcinoma↓(Redova et al., 2012)
hsa-miR-27a	Type 1 diabetes↑(Nielsen et al., 2012)
hsa-miR-29a	Type 1 diabetes↑(Nielsen et al., 2012), active pulmonary tuberculosis ↑(Fu et al., 2011), colorectal cancer↑(Huang et al., 2010)
hsa-miR-191	Type 2 diabetes↓(Zampetaki et al., 2010)
hsa-miR-223	Nasopharyngeal carcinoma↑(Zeng et al., 2012), Systemic lupus erythematosus↑(Wang et al., 2012a), gastric cancer↑(Li et al., 2010) Hepatocellular carcinoma↑(Qi et al., 2011; Xu et al., 2011), Type 2 diabetes↓(Zampetaki et al., 2010), Sepsis↓(Wang et al., 2010a)
hsa-miR-328	Acute myocardial infarction↓(Wang et al., 2011)
hsa-miR-21	Breast cancer↑(Si et al., 2013), aortic stenos↑(Villar et al., in press), esophageal squamous cell carcinoma↑(Komatsu et al., 2011) Non-small cell lung cancer↑(Wei et al., 2011), gastric cancer↑(Li et al., 2010; Zheng et al., 2011-2012)
hsa-miR-106b	Gastric cancer↑(Tsujiura et al., 2010)
hsa-miR-20b	Non-small cell lung cancer↓(Silva et al., 2011)
hsa-miR-17	Nasopharyngeal carcinoma↓(Zeng et al., 2012)
hsa-miR-20a	Non-small cell lung cancer↓(Silva et al., 2011)
hsa-miR-24	Type 1 diabetes↑(Nielsen et al., 2012), Type 2 diabetes ↓(Zampetaki et al., 2010)
hsa-miR-106a	Gastric cancer↑(Tsujiura et al., 2010)
hsa-miR-126	Acute myocardial infarction↑(Long et al., 2012a), Type 2 diabetes ↓(Zampetaki et al., 2010)
hsa-miR-16	Hepatocellular carcinoma↓(Qu et al., 2011)
hsa-miR-25	Type 1 diabetes↑(Nielsen et al., 2012)
hsa-miR-195	Acute myocardial infarction↑(Long et al., 2012b), breast cancer ↑(Heneghan et al., 2010)
hsa-miR-92a	Breast cancer↓(Si et al., 2013), colorectal cancer↑(Huang et al., 2010)

Conflict of interest statement

The authors declare that there are no conflicts of interest.

Acknowledgment

This work was supported by JSPS KAKENHI Grant Number 21659030 and a grant from the Smoking Research Foundation in Japan. We are grateful to Dr. Tomokazu Konishi of Akita Prefectural University for his valuable advice and help in PCA.

References

Ambros, V., 2001. microRNAs: tiny regulators with great potential. Cell 107, 823–826.
Bloomer, R.J., 2007. Decreased blood antioxidant capacity and increased lipid peroxidation in young cigarette smokers compared to nonsmokers: impact of dietary intake. Nutr. J. 6, 39.
Bryant, R.J., Pawlowski, T., Catto, J.W., Marsden, G., Vessella, R.L., Rhees, B., Kuslich, C., Visakorpi, T., Hamdy, F.C., 2012. Changes in circulating microRNA levels associated with prostate cancer. Br. J. Cancer 106, 768–774.
Chen, X., Ba, Y., Ma, L., Cai, X., Yin, Y., Wang, K., Guo, J., Zhang, Y., Chen, J., Guo, X., Li, Q., Li, X., 2008. Characterization of microRNAs in serum: a novel class of biomarkers for diagnosis of cancer and other diseases. Cell Res. 18, 997–1006.
Cookson, V.J., Bentley, M.A., Hogan, B.V., Horgan, K., Hayward, B.E., Hazelwood, L.D., Hughes, T.A., 2012. Circulating microRNA profiles reflect the presence of breast tumours but not the profiles of microRNAs within the tumours. Cell. Oncol. 35, 301–308.
Crosby, M.E., Devlin, C.M., Glazer, P.M., Calin, G.A., Ivan, M., 2009. Emerging roles of microRNAs in the molecular responses to hypoxia. Curr. Pharm. Des. 15, 3861–3866.
De Flora, S., Camoirano, A., Bagnasco, M., Bennicelli, C., van Zandwijk, N., Wigbout, G., Qian, G.S., Zhu, Y.R., Kensler, T.W., 1996. Smokers and urinary genotoxins: implications for selection of cohorts and modulation of endpoints in chemoprevention trials. J. Cell. Biochem. 25S, 92–98.
De Flora, S., Balansky, R., D'Agostini, F., Cartiglia, C., Longobardi, M., Steele, V.E., Izzotti, A., 2012. Smoke-induced microRNA and related proteome alterations. Modulation by chemopreventive agents. Int. J. Cancer 131, 2763–2773.
Duttagupta, R., Jiang, R., Gollub, J., Getts, R.C., Jones, K.W., 2011. Impact of cellular miRNAs on circulating miRNA biomarker signatures. PLoS One 6, e20769.
Fu, Y., Yi, Z., Wu, X., Li, J., Xu, F., 2011. Circulating microRNAs in patients with active pulmonary tuberculosis. J. Clin. Microbiol. 49, 4246–4251.
Graff, J.W., Powers, L.S., Dickson, A.M., Kim, J., Reisetter, A.C., Hassan, I.H., Kremens, K., Gross, T.J., Wilson, M.E., Monick, M.M., 2012. Cigarette smoking decreases global microRNA expression in human alveolar macrophages. PLoS One 7, e44066.
Hanke, M., Hoefig, K., Merz, H., Feller, A.C., Kausch, I., Jocham, D., Warnecke, J.M., Sczakiel, G., 2010. A robust methodology to study urine microRNA as tumor marker: microRNA-126 and microRNA-182 are related to urinary bladder cancer. Urol. Oncol. 28, 655–661.
He, L., Hannon, G.L., 2004. MicroRNAs: small RNAs with a big role in gene regulation. Nat. Rev. Genet. 5, 522–531.

Heneghan, H.M., Miller, N., Kelly, R., Newell, J., Kerin, M.J., 2010. Systemic miRNA-195 differentiates breast cancer from other malignancies and is a potential biomarker for detecting noninvasive and early stage disease. Oncologist 15, 673–682.

Higgins, M.W., Keller, J.B., Landis, J.R., Beaty, T.H., Burrows, B., Demets, D., Diem, J.E., Higgins, I.T., Lakatos, E., Lebowitz, M.D., 1984. Risk of chronic obstructive pulmonary disease. Collaborative assessment of the validity of the Tecumseh index of risk. Am. Rev. Respir. Dis. 130, 380–385.

Hoffmann, D., Hoffmann, I., El-Bayoumy, K., 2001. The less harmful cigarette: a controversial issue. A tribute to Ernst L. Wynder. Chem. Res. Toxicol. 14, 767–790.

Holbrook, J.H., Grundy, S.M., Hennekens, C.H., Kannel, W.B., Strong, J.P., 1984. Cigarette smoking and cardiovascular diseases. A statement for health professionals by a task force appointed by the steering committee of the American Heart Association. Circulation 70, 1114A–1117A.

Huang, Z., Huang, D., Ni, S., Peng, Z., Sheng, W., Du, X., 2010. Plasma microRNAs are promising novel biomarkers for early detection of colorectal cancer. Int. J. Cancer 127, 118–126.

Izzotti, A., Calin, G.A., Arrigo, P., Steele, V.E., Croce, C.M., De Flora, S., 2009a. Downregulation of microRNA expression in the lungs of rats exposed to cigarette smoke. FASEB J. 23, 806–812.

Izzotti, A., Calin, G.A., Steele, V.E., Croce, C.M., De Flora, S., 2009b. Relationships of microRNA expression in mouse lung with age and exposure to cigarette smoke and light. FASEB J. 23, 3243–3250.

Izzotti, A., Larghero, P., Longobardi, M., Cartiglia, C., Camoirano, A., Steele, V.E., De Flora, S., 2011. Dose-responsiveness and persistence of microRNA expression alterations induced by cigarette smoke in mouse lung. Mutat. Res. 717, 9–16.

Ji, J., Shi, J., Budhu, A., Yu, Z., Forgues, M., Roessler, S., Ambs, S., Chen, Y., Meltzer, P.S., Croce, C.M., Qin, L.X., Man, K., 2009. MicroRNA expression, survival, and response to interferon in liver cancer. N. Engl. J. Med. 361, 1437–1447.

Kanemaru, H., Fukushima, S., Yamashita, J., Honda, N., Oyama, R., Kakimoto, A., Masuguchi, S., Ishihara, T., Inoue, Y., Jinnin, M., Ihn, H., 2011. The circulating microRNA-221 level in patients with malignant melanoma as a new tumor marker. J. Dermatol. Sci. 61, 187–193.

Komatsu, S., Ichikawa, D., Takeshita, H., Tsujiura, M., Morimura, R., Nagata, H., Kosuga, T., Iitaka, D., Konishi, H., Shiozaki, A., Fujiwara, H., Okamoto, K., Otsuji, E., 2011. Circulating microRNAs in plasma of patients with oesophageal squamous cell carcinoma. Br. J. Cancer 105, 104–111.

Lee, Y., El Andaloussi, S., Wood, M.J., 2012. Exosomes and microvesicles: extracellular vesicles for genetic information transfer and gene therapy. Hum. Mol. Genet. 21, R125–R134.

Li, B.S., Zhao, Y.L., Guo, G., Li, W., Zhu, E.D., Luo, X., Mao, X.H., Zou, Q.M., Yu, P.W., Zuo, Q.F., Li, N., Tang, B., Liu, K.Y., Xiao, B., 2010. Plasma microRNAs, miR-223, miR-21 and miR-218, as novel potential biomarkers for gastric cancer detection. PLoS One 7, e41629.

Liang, Y., Ridzon, D., Wong, L., Chen, C., 2007. Characterization of microRNA expression profiles in normal human tissues. BMC Genomics 8, 166.

Long, G., Wang, F., Duan, Q., Chen, F., Yang, S., Gong, W., Wang, Y., Chen, C., Wang, D.W., 2012a. Human circulating microRNA-1 and microRNA-126 as potential novel indicators for acute myocardial infarction. Int. J. Biol. Sci. 8, 811–818.

Long, G., Wang, F., Duan, Q., Yang, S., Chen, F., Gong, W., Yang, X., Wang, Y., Chen, C., Wang, D.W., 2012b. Circulating miR-30a, miR-195 and let-7b associated with acute myocardial infarction. PLoS One 7, e50926.

Maccani, M.A., Avissar-Whiting, M., Banister, C.E., McGonnigal, B., Padbury, J.F., Marsit, C.J., 2010. Maternal cigarette smoking during pregnancy is associated with downregulation of miR-16, miR-21, and miR-146a in the placenta. Epigenetics 5, 583–589.

Mahn, R., Heukamp, L.C., Rogenhofer, S., von Ruecker, A., Müller, S.C., Ellinger, J., 2011. Circulating microRNAs (miRNA) in serum of patients with prostate cancer. Urology 77, 1265.e9–1265.e16.

Meder, B., Keller, A., Vogel, B., Haas, J., Sedaghat-Hamedani, F., Kayvanpour, E., Just, S., Borries, A., Rudloff, J., Leidinger, P., Meese, E., Katus, H.A., Rottbauer, W., 2011. MicroRNA signatures in total peripheral blood as novel biomarkers for acute myocardial infarction. Basic Res. Cardiol. 106, 13–23.

Meltzer, P.S., 2005. Cancer genomics: small RNAs with big impacts. Nature 435, 745–746.

Michael, A., Bajracharya, S.D., Yuen, P.S., Zhou, H., Star, R.A., Illei, G.G., Alevizos, I., 2010. Exosomes from human saliva as a source of microRNA biomarkers. Oral Dis. 16, 34–38.

Mitchell, P.S., Parkin, R.K., Kroh, E.M., Fritz, B.R., Wyman, S.K., Pogosova-Agadjanyan, E.L., Peterson, A., Noteboom, J., O'Briant, K.C., Allen, A., Lin, D.W., Urban, N., Drescher, C.W., Knudsen, B.S., Stirewalt, D.L., Gentleman, R., Vessella, R.L., Nelson, P.S., Martin, D.B., Tewari, M., 2008. Circulating microRNAs as stable blood-based markers for cancer detection. Proc. Natl. Acad. Sci. U. S. A. 105, 10513–10518.

Nakajima, M., Yamamoto, T., Kuroiwa, Y., Yokoi, T., 2000. Improved highly sensitive method for determination of nicotine and cotinine in human plasma by high-performance liquid chromatography. J. Chromatogr. B Biomed. Sci. Appl. 742, 211–215.

Nielsen, L.B., Wang, C., Sørensen, K., Bang-Berthelsen, C.H., Hansen, L., Andersen, M.L., Hougaard, P., Juul, A., Zhang, C.Y., Pociot, F., Mortensen, H.B., 2013. Circulating levels of microRNA from children with newly diagnosed type 1 diabetes and healthy controls: evidence that miR-25 associates to residual β-cell function and glycaemic control during disease progression. Exp. Diabetes Res (2012, Article ID 896362).

Olivieri, F., Antonicelli, R., Lorenzi, M., D'Alessandra, Y., Lazzarini, R., Santini, G., Spazzafumo, L., Lisa, R., La Sala, L., Galeazzi, R., Recchioni, R., Testa, R., Pompilio, G., Capogrossi, M.C., Procopio, A.D., 2013. Diagnostic potential of circulating miR-499-5p in elderly patients with acute non ST-elevation myocardial infarction. Int. J. Cardiol. http://dx.doi.org/10.1016/j.ijcard.2012.11.103 (in press).

Park, N.J., Zhou, H., Elashoff, D., Henson, B.S., Kastratovic, D.A., Abemayor, E., Wong, D.T., 2009. Salivary microRNA: discovery, characterization, and clinical utility for oral cancer detection. Clin. Cancer Res. 15, 5473–5477.

Pu, X.X., Huang, G.L., Guo, H.Q., Guo, C.C., Li, H., Ye, S., Ling, S., Jiang, L., Tian, Y., Lin, T.Y., 2010. Circulating miR-221 directly amplified from plasma is a potential diagnostic and prognostic marker of colorectal cancer and is correlated with p53 expression. J. Gastroenterol. Hepatol. 25, 1674–1680.

Qi, P., Cheng, S.Q., Wang, H., Li, N., Chen, Y.F., Gao, C.F., 2011. Serum microRNAs as biomarkers for hepatocellular carcinoma in Chinese patients with chronic hepatitis B virus infection. PLoS One 6, e28486.

Qu, K.Z., Zhang, K., Li, H., Afdhal, N.H., Albitar, M., 2011. Circulating microRNAs as biomarkers for hepatocellular carcinoma. J. Clin. Gastroenterol. 45, 355–360.

Redova, M., Poprach, A., Nekvindova, J., Iliev, R., Radova, L., Lakomy, R., Svoboda, M., Vyzula, R., Slaby, O., 2012. Circulating miR-378 and miR-451 in serum are potential biomarkers for renal cell carcinoma. J. Transl. Med. 10, 55.

Reid, G., Kirschner, M.B., van Zandwijk, N., 2011. Circulating microRNAs: association with disease and potential use as biomarkers. Crit. Rev. Oncol. Hematol. 80, 193–208.

Schembri, F., Sridhar, S., Perdomo, C., Gustafson, A.M., Zhang, X., Ergun, A., Lu, J., Liu, G., Zhang, X., Bowers, J., Vaziri, C., Ott, K., Sensinger, K., Collins, J.J., Brody, J.S., Getts, R., Lenburg, M.E., Spira, A., 2009. MicroRNAs as modulators of smoking-induced gene expression changes in human airway epithelium. Proc. Natl. Acad. Sci. U. S. A. 106, 2319–2324.

Shende, V.R., Goldrick, M.M., Ramani, S., Earnest, D.J., 2011. Expression and rhythmic modulation of circulating microRNAs targeting the clock gene *Bmal1* in mice. PLoS One 6, e22586.

Shields, P.G., 1999. Molecular epidemiology of lung cancer. Ann. Oncol. 5, S7–S11.

Si, H., Sun, X., Chen, Y., Cao, Y., Chen, S., Wang, H., Hu, C., 2013. Circulating microRNA-92a and microRNA-21 as novel minimally invasive biomarkers for primary breast cancer. J. Cancer Res. Clin. Oncol 139, 223–229.

Silva, J., García, V., Zaballos, Á., Provencio, M., Lombardía, L., Almonacid, L., García, J.M., Domínguez, G., Peña, C., Diaz, R., Herrera, M., Varela, A., Bonilla, F., 2011. Vesicle-related microRNAs in plasma of nonsmall cell lung cancer patients and correlation with survival. Eur. Respir. J. 37, 617–623.

Tsujiura, M., Ichikawa, D., Komatsu, S., Shiozaki, A., Takeshita, H., Kosuga, T., Konishi, H., Morimura, R., Deguchi, K., Fujiwara, H., Okamoto, K., Otsuji, E., 2010. Circulating microRNAs in plasma of patients with gastric cancers. Br. J. Cancer 102, 1174–1179.

Ulrik, C.S., Lange, P., 2001. Cigarette smoking and asthma. Monaldi Arch. Chest Dis. 56, 349–353.

Vickers, K.C., Palmisano, B.T., Shoucri, B.M., Shamburek, R.D., Remaley, A.T., 2011. MicroRNAs are transported in plasma and delivered to recipient cells by high-density lipoproteins. Nat. Cell Biol. 13, 423–433.

Villar, A.V., García, R., Merino, D., Llano, M., Cobo, M., Montalvo, C., Martín-Durán, R., Hurlé, M.A., Nistal, J.F., 2013. Myocardial and circulating levels of microRNA-21 reflect left ventricular fibrosis in aortic stenosis patients. Int. J. Cardiol. http://dx.doi.org/10.1016/j.ijcard.2012.07.021 (in press).

Wang, K., Zhang, S., Marzolf, B., Troisch, P., Brightman, A., Hu, Z., Hood, L.E., Galas, D.J., 2009. Circulating microRNAs, potential biomarkers for drug-induced liver injury. Proc. Natl. Acad. Sci. U. S. A. 106, 4402–4407.

Wang, J.F., Yu, M.L., Yu, G., Bian, J.J., Deng, X.M., Wan, X.J., Zhu, K.M., 2010a. Serum miR-146a and miR-223 as potential new biomarkers for sepsis. Biochem. Biophys. Res. Commun. 394, 184–188.

Wang, K., Zhang, S., Weber, J., Baxter, D., Galas, D.J., 2010b. Export of microRNAs and microRNA-protective protein by mammalian cells. Nucleic Acids Res. 38, 7248–7259.

Wang, R., Li, N., Zhang, Y., Ran, Y., Pu, J., 2011. Circulating microRNAs are promising novel biomarkers of acute myocardial infarction. Intern. Med. 50, 1789–1795.

Wang, H., Peng, W., Ouyang, X., Li, W., Dai, Y., 2012a. Circulating microRNAs as candidate biomarkers in patients with systemic lupus erythematosus. Transl. Res. 160, 198–206.

Wang, K., Yuan, Y., Cho, J.H., McClarty, S., Baxter, D., Galas, D.J., 2012b. Comparing the microRNA spectrum between serum and plasma. PLoS One 7, e41561.

Wei, J., Gao, W., Zhu, C.J., Liu, Y.Q., Mei, Z., Cheng, T., Shu, Y.Q., 2011. Identification of plasma microRNA-21 as a biomarker for early detection and chemosensitivity of non-small cell lung cancer. Chin. J. Cancer 30, 407–414.

Xu, J., Wu, C., Che, X., Wang, L., Yu, D., Zhang, T., Huang, L., Li, H., Tan, W., Wang, C., Lin, D., 2011. Circulating microRNAs, miR-21, miR-122, and miR-223, in patients with hepatocellular carcinoma or chronic hepatitis. Mol. Carcinog. 50, 136–142.

Yamaguchi, Y., Haginaka, J., Morimoto, S., Fujijoka, Y., Kunimoto, M., 2005. Facilitated nitration and oxidation of LDL in cigarette smokers. Eur. J. Clin. Invest. 35, 186–193.

Yamanaka, H., Nakajima, M., Nishimura, K., Yoshida, R., Fukami, T., Katoh, M., Yokoi, T., 2004. Metabolic profile of nicotine in subjects whose *CYP2A6* gene is deleted. Eur. J. Pharm. Sci. 22, 419–425.

Yamaura, Y., Nakajima, M., Takagi, S., Fukami, T., Tsuneyama, K., Yokoi, T., 2012. Plasma microRNA profiles in rat models of hepatocellular injury, cholestasis, and steatosis. PLoS One 7, e30250.

Yu, S., Liu, Y., Wang, J., Guo, Z., Zhang, Q., Yu, F., Zhang, Y., Huang, K., Li, Y., Song, E., Zheng, X.L., Xiao, H., 2012. Circulating microRNA profiles as potential biomarkers for diagnosis of papillary thyroid carcinoma. J. Clin. Endocrinol. Metab. 97, 2084–2092.

Zampetaki, A., Kiechl, S., Drozdov, I., Willeit, P., Mayr, U., Prokopi, M., Mayr, A., Weger, S., Oberhollenzer, F., Bonora, E., Shah, A., Willeit, J., Mayr, M., 2010. Plasma microRNA profiling reveals loss of endothelial miR-126 and other microRNAs in type 2 diabetes. Circ. Res. 107, 810–817.

Zeng, X., Xiang, J., Wu, M., Xiong, W., Tang, H., Deng, M., Li, X., Liao, Q., Su, B., Luo, Z., Zhou, Y., Zhou, M., Zeng, Z., Li, X., Shen, S., Shuai, C., Li, G., Fang, J., Peng, S., 2012. Circulating miR-17, miR-20a, miR-29c, and miR-223 combined as non-invasive biomarkers in nasopharyngeal carcinoma. PLoS One 7, e46367.

Zheng, Y., Cui, L., Sun, W., Zhou, H., Yuan, X., Huo, M., Chen, J., Lou, Y., Guo, J., 2011–2012. MicroRNA-21 is a new marker of circulating tumor cells in gastric cancer patients. Cancer Biomark. 10, 71–77.

TOXICOLOGICAL SCIENCES 136(1), 250–263 2013
doi:10.1093/toxsci/kft184
Advance Access publication August 28, 2013

A Novel Mouse Model for Phenytoin-Induced Liver Injury: Involvement of Immune-Related Factors and P450-Mediated Metabolism

Eita Sasaki,* Kentaro Matsuo,* Azumi Iida,* Koichi Tsuneyama,† Tatsuki Fukami,* Miki Nakajima,* and Tsuyoshi Yokoi*,[1,2]

*Drug Metabolism and Toxicology, Faculty of Pharmaceutical Sciences, Kanazawa University, Kanazawa 920–1192, Japan; and †Department of Diagnostic Pathology, Graduate School of Medicine and Pharmaceutical Science for Research, University of Toyama, Toyama 930-0194, Japan

[1]Present address: Department of Drug Safety Sciences Nagoya University Graduate School of Medicine, Nagoya, 466-8550, Japan
[2]To whom correspondence should be addressed at Department of Drug Safety Sciences Nagoya University Graduate School of Medicine 65 Tsurumai-cho, Showa-ku, Nagoya, 466-8550, Japan. Fax: +81-76-234-4407. E-mail: tyokoi@p.kanazawa-u.ac.jp.

Received May 19, 2013; accepted August 19, 2013

Drug-induced liver injury is an important issue for drug development and clinical drug therapy; however, in most cases, it is difficult to predict or prevent these reactions due to a lack of suitable animal models and the unknown mechanisms of action. Phenytoin (DPH) is an anticonvulsant drug that is widely used for the treatment of epilepsy. Some patients who are administered DPH will suffer symptoms of drug-induced liver injury characterized by hepatic necrosis. DPH-induced liver injury occurs in 1 in 1000 or 1 in 10 000 patients. Clinically, 75% of patients who develop liver injury develop a fever and 63% develop a rash. In this study, we established a mouse model for DPH-induced liver injury and analyzed the mechanisms for hepatotoxicity in the presence of immune-related or inflammation-related factors and metabolic activation. Female C57BL/6 mice were administered DPH for 5 days in combination with L-buthionine-S,R-sulfoximine. Then, the plasma alanine aminotransferase (ALT) levels were increased, hepatic lesions were observed during the histological evaluations, the hepatic glutathione levels were significantly reduced, and the oxidative stress marker levels were significantly increased. The inhibition of cytochrome P450-dependent oxidative metabolism significantly suppressed the elevated plasma ALT levels and depleted hepatic glutathione. Among the innate immune factors, the hepatic mRNA levels of NACHT, LRR, pyrin domain-containing protein 3, interleukin-1β, and damage-associated molecular patterns were significantly increased. Prostaglandin E_1 treatment ameliorated the hepatic injury caused by DPH. In conclusion, cytochrome P450-dependent metabolic activation followed by the stimulation of the innate immune responses is involved in DPH-induced liver injury.

Key Words: **phenytoin; IL-17; hepatotoxicity; glutathione; mouse model.**

Drug-induced liver injury is a serious issue for new drug candidates and for products currently on the market. Phenytoin (5,5-diphenylhydantoin, DPH) is an anticonvulsant drug that is widely used for the treatment of epilepsy. A fraction of patients administered DPH will suffer symptoms of drug hypersensitivity, typically characterized by a rash, lymphadenopathy, fever, and if the drug continues to be used, drug-induced liver injury (Dhar *et al.*, 1974; Haruda, 1979; Taylor *et al.*, 1984). Hepatic necrosis with a prominent inflammatory response occurs 1–8 weeks after exposure in between 1 in 1000 and 1 in 10 000 patients who receive DPH (Mullick and Ishak, 1980). Therefore, DPH-induced liver injury is generally recognized as idiosyncratic.

Generally, reactive metabolite formation followed by covalent binding may be associated with idiosyncratic toxicity via immune mechanisms (Spielberg *et al.*, 1981). The major metabolic pathway of DPH has been well documented. DPH is hydroxylated by cytochrome P450 (CYP) enzymes to form its phenol metabolite, 5-(*p*-hydroxyphenyl-),5-phenylhydantoin (HPPH). HPPH can be further oxidized to form the DPH catechol (Munns *et al.*, 1997). A number of *in vitro* studies show that the DPH catechol can form protein adducts in the liver microsomes of humans and mice and that DPH catechol formation is catalyzed primarily by CYP2C19 and CYP2C9 in humans (Cuttle *et al.*, 2000) and CYP2C11 in rats (Yamazaki *et al.*, 2001). Covalent bond formation is suppressed when low molecular weight thiols such as glutathione (GSH) and cysteine are present in mice microsomes (Roy and Snodgrass, 1990). Considering these *in vitro* reports, we suspect that the CYP-produced reactive metabolite of DPH covalently binding to hepatic proteins may be responsible for DPH-induced idiosyncratic toxicity. However, there are currently no *in vivo* studies on hepatic GSH content or P450 oxidization metabolism in DPH-induced liver injury due to a lack of an appropriate animal model.

Studies have shown that DPH may generate reactive oxygen species (ROS). For example, antioxidants such as superoxide dismutase (SOD), catalase, and GSH confer protection against DPH embryopathy *in vitro* (Winn and Wells, 1995) and *in vivo* (Winn and Wells, 1999). Recently, ROS have been proposed to

play an important role in the activation of the NACHT-, LRR-, and pyrin domain-containing protein 3 (NALP3) inflammasome (Bryant and fitzgerald, 2009; Martinon *et al.*, 2009). The NALP3 inflammasome generates mature interleukin (IL)-1β via proteolytic pathways, and mature IL-1β engages IL-1R-harboring cells and promotes inflammatory responses (Latz, 2010; Schroder and Tschopp, 2010).

The most frequent mechanism of drug-induced liver injury is the CYP-dependent formation of reactive metabolites that cause cell death or immune reactions that amplify tissue trauma. Necrotic cell death triggers a release of damage-associated molecular patterns (DAMPs), such as the S100 protein and high-mobility group box 1 (HMGB1), which activate innate immune cells (Bianchi, 2007; Scaffidi *et al.*, 2002). The activation of innate immune cells by DAMPs occurs through toll-like receptors (TLRs; Schwabe *et al.*, 2006). Cytokines and chemokines, followed by inflammation or the infiltration of lymphocytes to hepatocytes, are involved in immune-mediated hepatotoxicity and are predominantly secreted by immune cells such as T lymphocytes and macrophages (Kita *et al.*, 2001; Oo and Adams, 2010). Cytokine production is induced by the following transcriptional factors: T-box expressed in T cells (T-bet) induces the secretion of interferon-γ and IL-12; GATA-binding domain-3 (GATA-3) induces IL-4, IL-5, and IL-13 production; and retinoid-related orphan receptor (ROR)-γt is indispensable for the differentiation of Th17 cells, which secrete primarily IL-17 (Kidd, 2003; Langrish *et al.*, 2005; Steinman, 2007).

A number of groups including our own have also recently applied a GSH-depleted animal model to both the evaluation of hepatotoxic potential and the analysis of hepatotoxicity in several drugs that produce reactive metabolites, such as acetaminophen (Watanabe *et al.*, 2003), ticlopidine (Shimizu *et al.*, 2011), and methimazole (Kobayashi *et al.*, 2012). In an animal system depleted of GSH by a well-known GSH synthesis inhibitor, L-buthionine-S,R-sulfoximine (BSO), the tissue GSH levels were significantly reduced without any overt toxicity (Watanabe *et al.*, 2003) or any effects on the hepatic microsomal and cytosolic enzymes responsible for drug metabolism (Drew and Miners, 1984; Watanabe *et al.*, 2003).

In this study, we successfully established a DPH-induced liver injury mouse model using wild-type mice treated with DPH and BSO for 5 days. Our data suggest that DPH metabolism by CYPs and the hepatic GSH content are both involved in DPH-induced liver injury. Furthermore, the inflammation and immune factors believed to be involved in DPH-induced liver injury were investigated.

MATERIALS AND METHODS

Chemicals. DPH, BSO, and mephenytoin were purchased from Wako Pure Chemical Industries (Osaka, Japan); 1-aminobenzotriazole (ABT) was purchased from the Tokyo Chemical Industry (Tokyo, Japan). Eritoran was kindly provided by the Eisai Co. (Tokyo, Japan). Prostaglandin E_1 (PGE_1) was purchased from Nippon Chemiphar (Tokyo, Japan). The Fuji DRI-CHEM slides for GPT/ALT-PIII, GOT/AST-PIII, and TBIL-PIII used to measure alanine aminotransferase (ALT), aspartate aminotransferase (AST), and total bilirubin (T-Bil), respectively, were from Fujifilm (Tokyo, Japan). RNAiso was obtained from Nippon Gene (Tokyo, Japan), ReverTraAce was obtained from Toyobo (Tokyo, Japan), and random hexamers and SYBR Premix EX Taq were from Takara (Osaka, Japan). All primers were commercially synthesized at Hokkaido System Sciences (Sapporo, Japan). The monoclonal anti-mouse IL-17 antibody and the monoclonal rat IgG2a isotype used as a control were obtained from R&D Systems (Abingdon, UK). The rabbit polyclonal antibody against myeloperoxidase (MPO) was obtained from DAKO (Carpinteria, CA). The Ready-SET-GO! Mouse IL-17 ELISA Kit and the Mouse IL-1β ELISA Kit were purchased from eBioscience (San Diego, CA). The chicken anti-HMGB1 polyclonal antibody, chicken polyclonal IgY isotype, and HMGB1 ELISA Kit II were obtained from the Sino-Test Corporation (Tokyo, Japan). The other chemicals used were of analytical or the highest commercially available grade.

DPH and BSO treatments. Female C57BL/6JmsSLC mice (8 weeks old, 16–21 g) were obtained from SLC Japan (Hamamatsu, Japan). The mice were housed in a controlled environment at 23°C ± 1°C and 50% ± 10% humidity and with a 12-h light/12-h dark cycle in the institution's animal facility with ad libitum access to food and water. The animals were acclimatized before being used in the experiments. In this study, female C57BL/6J mice were used because female mice showed higher sensitivity to DPH-induced liver injury than male mice (data not shown). Repeated administration of DPH orally at a dose of 100 mg/kg for 6 days caused high mortality (60% of mice were dead on days 1 through 6). We speculated that this high mortality was caused by the pharmacological effects of DPH. DPH is known to induce CYPs (Cyps) in humans (Chaudhry *et al.*, 2010; Fleishaker *et al.*, 1995) and mice (Hagemeyer *et al.*, 2010). Thus, repeated administration of DPH increased DPH metabolism, contributing to the reduction of its pharmacological effects. However, the administration of DPH at a dose of 100 mg/kg for 6 days caused high mortality on days 1 and 2 due to its pharmacological effects. This phenomenon is partially explained by the fact that on days 1 and 2, induction of hepatic Cyps by DPH did not occur or was insufficient. Thus, we thought that the dose amount of DPH on days 1 and 2 should be under 100 mg/kg to reduce mortality. Therefore, we employed a dosing regimen as follows. First, 50 mg/kg of DPH was IP injected for the first 2 days. In this step, we expected to induce the hepatic Cyps by DPH. On days 3 through 5, 100 mg/kg of DPH was orally administered. In this step, we expected that the expression of hepatic Cyps had been induced by 50 mg/kg of DPH during the first 2 days of IP administration. In this dosing regimen, the mortality rate was 10%–20% on days 1 through 5. Thus, the dosage of DPH was increased to 100 mg/kg on days 3 through 5. BSO is generally administered IP. To avoid unexpected adverse interactions between DHP and BSO, we changed the dosing route of DPH on days 3 through 5. Finally, in this study, the mice were IP administered DPH in corn oil at a dose of 50 mg/kg for 2 days followed by oral administration of 100 mg/kg on days 3 through 5. BSO in saline was IP injected at a dose of 700 mg/kg 1 h prior to each DPH administration as reported by Shimizu *et al.* (2011). As a control, mice were injected with corn oil or saline, which were used as the vehicles for DPH and BSO, respectively. To determine the time-dependent changes in the plasma ALT levels, the mice were anesthetized with ether, and then blood was collected at 0 and 6 h after DPH administration on days 1 through 4 and 0, 3, 6, 24, and 48 h after the final DPH administration. Each group included 4–6 mice. At 72 h after the final DPH administration (final time point for blood collection), the blood samples were collected from the inferior vena cava for biochemical analyses. For measurement of the hepatic mRNA expression of immune- and inflammation-related factors, hepatic GSH content, protein carbonyl content, and histopathological analysis, individual mice were investigated at 24 h before (–24) and at 0, 1.5, 3, 6, 12, or 24 h after the final DPH administration. The blood samples were collected from the inferior vena cava for measurement of plasma cytokine levels. A portion of the hepatic left lobe was excised and fixed in 10% neutral buffered formalin for the histopathological examinations. The remaining liver was frozen in liquid nitrogen and stored at −80°C until use for the measurement of mRNA

expression levels, protein carbonyl content, and GSH content. Each treatment group included 3–5 mice in each time point. As a negative control, we chose mephenytoin as a structural homologue of DPH and with similar pharmacological effects to DPH. In addition, mephenytoin-induced liver injury has a low incidence compared with DPH (Zimmerman, 1999). The mice were administered mephenytoin in corn oil using the same dosing regimen as that used for DPH and BSO. To investigate the importance of the repeated administration for developing DPH-induced liver injury, we conducted a single-administration study. To investigate whether liver injury does not occur, the mice were either IP given 50 mg/kg or 100 mg/kg DPH, or they were orally given 100 or 200 mg/kg DPH and euthanized 24 h after drug administration. BSO (700 mg/kg) was IP injected 1 h prior to DPH treatment. A portion of each excised liver was fixed in a 10% formalin neutral buffer solution and used for immunohistochemistry. The degree of liver injury was assessed by hematoxylin and eosin staining and MPO staining. The plasma ALT, AST, and T-Bil levels were measured using DRI-CHEM (Fujifilm). The animals were treated and maintained in accordance with the National Institutes of Health Guide for Animal Welfare of Japan, and the animal protocols were approved by the Institutional Animal Care and Use Committee of Kanazawa University, Japan.

Treatment with ABT. One hour prior to the final DPH treatment, the mice were IP injected with ABT (100 mg/kg in saline) according to the previous studies (Shimizu et al., 2009, 2011). The vehicle was used as a control.

GSH assay. The mouse livers were homogenized in ice-cold 5% sulfosalicylic acid and centrifuged at 8000 × g for 10 min. The supernatant total GSH and glutathione disulfide (GSSG) concentration was measured as previously described (Tietze, 1969). The GSH levels were calculated from the difference between the total GSH and the GSSG concentration.

Protein carbonyl content. Increased protein carbonyls are a stable indicator of oxidative stress. The protein carbonyl content of the liver homogenate was measured using a Protein Carbonyl ELISA kit (Enzo LifeScience, New York). The assay was performed according to the manufacturer's instructions.

Real-time reverse transcription (RT)-PCR. RNA from mouse liver was isolated using RNAiso (Nippon Gene, Tokyo, Japan) according to the manufacturer's instructions. The mRNA levels of S100A8, S100A9, TLR2, TLR4, TLR9, receptor for advanced glycation end products (RAGE), NALP3, IL-1β, IL-23 p19, IL-6, GATA-3, RORγt, forkhead box P3 (Foxp3), Fas, FasL, T-bet, macrophage inflammatory protein-2 (MIP-2), and monocyte chemoattractant protein-1 (MCP-1) were quantified using real-time RT-PCR. For the RT step, total RNA (10 μg) and 150 ng of random hexamers were mixed and incubated at 70°C for 10 min. The RNA solution was added to a reaction mixture containing 100 units of ReverTra Ace, reaction buffer, and 0.5mM deoxyribonucleotide triphosphates at a final volume of 40 μl. The resulting reaction mixture was incubated at 30°C for 10 min, 42°C for 1 h, and heated to 98°C for 10 min to inactivate the enzyme. Real-time RT-PCR was performed using the MX3000P instrument (Stratagene, La Jolla, California). The PCR mixture contained 1 μl of template cDNA, SYBR Premix Ex Taq solution, and 8 pmol each of forward and reverse primers. The amplified products were monitored directly by measuring the increase of the SYBR Green I (Molecular Probes, Eugene, Oregon) dye intensity. The primer sequences are shown in Table 1.

Measurement of plasma HMGB1, IL-17, and IL-1β levels. The plasma levels of HMGB1, IL-17, and IL-1β were measured by ELISA using the HMGB1 ELISA Kit II, a Ready-SET-GO! Mouse IL-17, and a Ready-SET-GO! Mouse IL-1β Kit, respectively, according to the manufacturers' instructions.

Administration of a TLR4 antagonist. The mice were IV treated with eritoran, a TLR4 antagonist (50 μg/mouse in 0.2 ml sterile saline), simultaneously with the final DPH treatment as previously described (Higuchi *et al.*, 2012). The vehicle was used as a control.

Administration of an anti-mouse IL-17 antibody or an anti-mouse HMGB1 antibody. In the IL-17 neutralization study, as described in our previous report (Higuchi *et al.*, 2012), the mice were IV treated with an anti-mouse IL-17 antibody (100 μg anti-mouse IL-17 antibody in 0.2 ml sterile PBS) 3 h after the final DPH treatment. As a control, rat IgG2a was used (100 μg rat IgG2a in 0.2 ml sterile PBS). In the HMGB1 neutralization study, the mice were IV treated with an anti-mouse HMGB1 antibody (200 μg anti-mouse HMGB1 antibody in 0.2 ml sterile PBS) simultaneously with the final DPH treatment. As a control, a chicken IgY isotype was used (200 μg chicken IgY in 0.2 ml sterile PBS).

Quantification of hepatic MPO-positive cells. The infiltration of neutrophils was assessed by immunostaining for MPO. A rabbit polyclonal antibody against MPO was used for the immunohistochemical staining of liver as previously described (Higuchi *et al.*, 2012). Three visual fields of ×400 magnification (0.1 mm^2 each) were randomly selected from each MPO-immunostained section. The total number of MPO-positive mononuclear cells from the 3 randomly selected visual fields was compared among the specimens.

Treatment with PGE1. Three hours after the final DPH treatment, the mice were IP given PGE_1 (at 50 μg/mouse in 0.5 ml sterile saline) as previously described (Higuchi *et al.*, 2012; Kobayashi *et al.*, 2009). The vehicle was used as a control.

Statistical analysis. The data are shown as the mean ± SEM. Statistical analyses of multiple groups were performed using a one-way ANOVA with the Dunnett's post hoc test to determine the significance of the differences between individual groups. Comparisons between 2 groups were carried out using a 2-tailed Student's *t* test. A value of $p < .05$ was considered statistically significant.

RESULTS

Development of a DPH-Induced Liver Injury in C57BL/6 Mice

DPH is widely used as an anticonvulsant drug and rarely causes hepatotoxicity with or without hypersensitivity. To study the mechanism of hepatotoxicity, we developed an animal model for DPH-induced liver injury in mice. The mice were IP given DPH at a dose of 50 mg/kg for 2 days and orally administered 100 mg/kg on days 3 through 5. BSO was given on all days. With this dosing regimen, the ALT levels were significantly increased after the final DPH treatment without a high fatality rate (Fig. 1A, mortality rate was 10%–20% on days 1 through 5). These hepatotoxic effects were observed in approximately 60% of the mice, and the others showed no or mild hepatotoxicity, resulting in large SEM values. Without BSO, the plasma ALT levels were much lower than those in the BSO-treated mice. No significant elevation of ALT levels was observed in mice treated with vehicle or BSO alone (Fig. 1A).

In a single-administration study, the female C57BL/6 mice were orally given DPH at a dose of 100 or 200 mg/kg in combination with BSO. The plasma ALT level was not affected by DPH treatment (Fig. 1B). Next, the mice were IP given DPH at a dose of 50 or 100 mg/kg in combination with BSO, resulting in no hepatotoxicity caused by DPH (Fig. 1B).

Mephenytoin, used as a negative control, did not induce hepatotoxicity under the same dosing regimen as DPH, even when combined with BSO, suggesting that the hepatotoxicity of DPH is independent of its pharmacological effects (Fig. 1C).

In the histopathological experiments, apoptosis and hepatocyte ballooning were observed at 24 h after the final DPH and BSO treatment (Fig. 1D). In addition, immunohistochemistry with an anti-MPO antibody demonstrated that a number of MPO-positive cells had infiltrated in DPH- and BSO-treated mice (Fig. 1D). The

TABLE 1.
Sequences of the Primers Used for Real-time RT-PCR Analyses

Genes		Sequences
FasL	FP	AGA AGG AAC TGG CAG AAC TC
	RP	GCG GTT CCA TAT GTG TCT TC
Foxp3	FP	CTA GCA GTC CAC TTC ACC AAG
	RP	GCT GCT GAG ATG TGA CTG TC
Gapdh	FP	AAA TGG GGT GAG GCC GGT
	RP	ATT GCT GAC AAT CTT GAG TGA
GATA-3	FP	GGA GGA CTT CCC CAA GAG CA
	RP	CAT GCT GGA AGG GTG GTG A
IL-1β	FP	GTT GAC GGA CCC CAA AAG AT
	RP	CAC ACA CCA GCA GGT TAT CA
IL-6	FP	CCA TAG CTA CCT GGA GTA CA
	RP	GGA AAT TGG GGT AGG AAG GA
IL-23 p19	FP	CCA GTG TGA AGA TGG TTG TG
	RP	CTA GTA GGG AGG TGT GAA GT
MIP-2	FP	AAG TTT GCC TTG ACC CTG AAG
	RP	ATC AGG TAC GAT CCA GGC TTC
MCP-1	FP	TGT CAT GCT TCT GGG CTT G
	RP	CCT CTC TCT TGA GCT TGG TG
NALP3	FP	GTT GAC GGA CCC CAA AAG AT
	RP	CAC ACA CCA GCA GGT TAT CA
RAGE	FP	GTG CTG GTT CTT GCT CTA TG
	RP	ATC GAC AAT TCC AGT GGC TG
ROR-γt	FP	ACC TCC ACT GCC AGC TGT GTG CTG TC
	RP	TCA TTT CTG CAC TTC TGC ATG TAG ACT GTC CC
S100A8	FP	GAG TGT CCT CAG TTT GTG CAG
	RP	TAG ACA TAT CCA GGG ACCCAG
S100A9	FP	GAT GGC CAA CAA AGC ACC TT
	RP	CCT CAA AGC TCA GCT GAT TG
T-bet	FP	TGC CCG AAC TAC AGT CAG GAA C
	RP	AGT GAC CTC GCC TGG TGA AAT G
TLR2	FP	GAA AAG ATG TCG TTC AAG GAG
	RP	TTG CTG AAG AGG ACT GTT ATG
TLR4	FP	TTC TTC TCC TGC CTG ACA CC
	RP	CCA TGC CAT GCC TTG TCT TC
TLR9	FP	ATT CTC TGC CGC CCA GTT TGT C
	RP	ACG GTT GGA GAT CAA GGA GAG G

Abbreviations: Foxp3, forkhead box P3; FP: forward primer; GATA-3, GATA-binding domain-3; IL, interleukin; MCP-1, monocyte chemoattractant protein-1; MIP-2, macrophage inflammatory protein-2; NALP3, NACHT-, LRR-, and pyrin domain-containing protein 3; RAGE, receptor for advanced glycation end products; ROR, retinoid-related orphan receptor; RP, reverse primer; T-bet, T-box expressed in T cells; TLR, toll-like receptor.

number of MPO-positive cells was significantly increased in mice given DPH or DPH plus BSO compared with vehicle-treated mice (Fig. 1E). However, liver section of DPH-alone-treated (without BSO) mice were often observed to have mild fat droplets but no apoptotic or ballooning cells, suggesting that the hepatic lesion mainly occurred in mice given both DPH and BSO. No histopathological difference was observed between the vehicle- and BSO-treated mice. Taken together, these results indicate that a DPH-induced liver injury mouse model was established.

Changes in Hepatic GSH and Oxidative Stress Marker Levels

The depletion of hepatic GSH by BSO was expected to exacerbate DPH-induced hepatotoxicity. Therefore, we investigated whether GSH is involved in the detoxification of DPH-induced liver injury. GSH levels were significantly decreased at all time points in mice given both DPH and BSO (Fig. 2A). In mice given only DPH, the GSH levels were significantly lower at 1.5, 3, 6, and 24 h after the final DPH treatment. These results suggest that DPH has the ability to deplete hepatic GSH, leading to the development of DPH-induced hepatotoxicity.

We measured hepatic GSSG, a biomarker of oxidative stress. Changes in hepatic GSSG levels showed a similar profile to that of GSH (Fig. 2A). The total glutathione (GSH+GSSG) levels were significantly lowered in mice treated with DPH alone and DPH and BSO together. The GSH/GSSG ratio, a biomarker of oxidative stress, was significantly lowered 1.5 h after the final DPH treatment in mice given both DPH and BSO. The hepatic protein carbonyl levels, a marker of oxidative stress, were significantly increased 6 h after the final DPH treatment in mice given both DPH and BSO but not in mice given only DPH or vehicle (Fig. 2B). These results suggest that oxidative stress is involved in DPH-induced liver injury and that GSH may have a protective role in DPH-induced liver injury.

Effect of the P450 Inhibitor

To investigate whether P450-mediated metabolism is involved in DPH-induced liver injury, mice were IP given ABT (100 mg/kg), a nonspecific inhibitor of P450, 1 h prior to the final DPH administration. In the ABT-treated mice, the elevated plasma ALT and AST levels were significantly suppressed (Fig. 3A). Treatment with ABT alone or ABT and BSO together (data not shown) did not result in any changes in the ALT or AST levels compared with the vehicle-treated mice.

To confirm the involvement of reactive intermediates in the DPH-induced liver injury, we measured the effects of ABT on the hepatic GSH and GSSG levels. The hepatic GSH depletion caused by DPH was significantly restored by ABT 24 h after the final DPH treatment (Fig. 3B). ABT alone did not change the GSH levels, suggesting that ABT itself does not affect the hepatic GSH levels at this dosing regimen. The hepatic total glutathione (GSH + GSSG) levels had a similar profile to that of GSH, suggesting that GSH may be consumed by P450-mediated reactive metabolites (Fig. 3B). These results suggest that P450-mediated metabolism is involved in DPH-induced liver injury.

Changes in the Expression Levels of DAMP-Related Factors

To investigate whether DAMPs and their receptors are involved in the onset of liver injury, time-dependent changes in the hepatic mRNA expression levels of TLR9, TLR4, TLR2, S100A9, S100A8, and RAGE were measured (Fig. 4A). The mRNA expression level of TLR2 was extremely variable in the treated mice, but it was significantly increased at some time points in response to either DPH or DPH plus BSO. The expression level of S100A8 mRNA was significantly increased

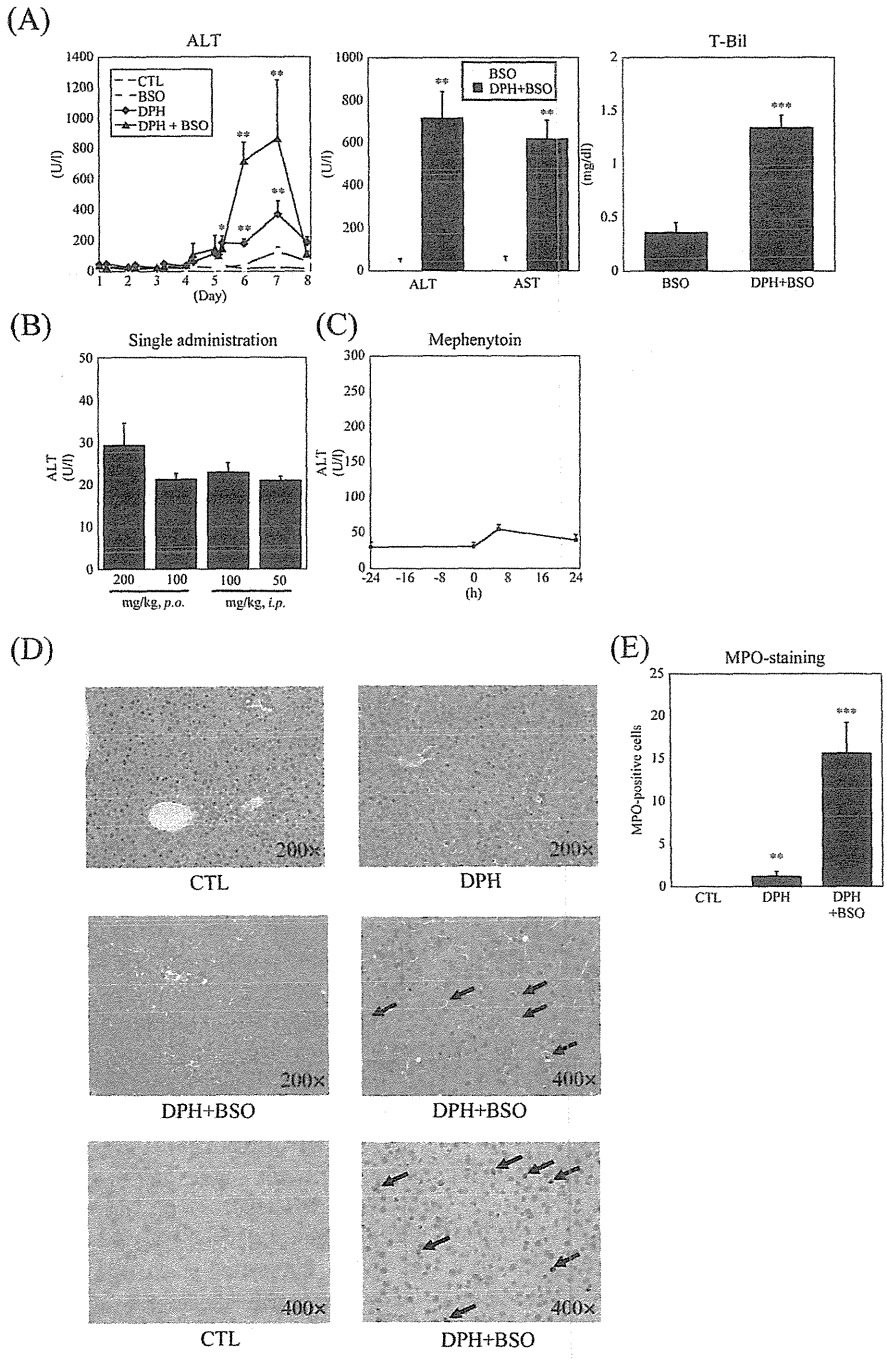

FIG. 1. Time-dependent changes in plasma ALT and AST levels in DPH-induced liver injury. A, Female C57BL/6 mice were IP given DPH at 50 mg/kg for 2 days followed by oral administration of 100 mg/kg DPH on days 3 through 5. BSO (700 mg/kg) was IP injected 1 h prior to each DPH administration. Each vehicle was used as a control. At 0 and 6 h after DPH administration on days 1–4 and at 0, 3, 6, 24, 48, and 72 h after the final DPH treatment, blood was collected to measure the plasma ALT levels. The days 6, 7, and 8 correspond to 24, 48, and 72 h after the final DPH treatment. In the second panel, the plasma ALT, AST, and T-Bil levels were measured 24 h after the final DPH treatment. The values represent the mean ± SEM of 4–6 animals. B, In a single-administration experiment, the mice were given an oral dose of DPH at 200 or 100 mg/kg and an IP injection of 100 or 50 mg/kg. BSO (700 mg/kg) was IP injected 1 h prior to the DPH treatment, and blood was collected 24 h after DPH administration. The values represent the mean ± SEM of 4 animals. C, As the negative control, the mice were given mephenytoin and BSO with the same dosing regimen as in (A). At 24 h before (−24) and 0, 6, and 24 h after the final mephenytoin treatment, blood was collected to measure the plasma ALT levels. Values represent the mean ± SEM of 4 animals. D, Liver tissue sections from 24 h after the final DPH treatment were stained with hematoxylin and eosin. Neutrophil infiltration was assessed by immunostaining for MPO. The arrows indicate apoptosis or MPO-positive cells. E, The number of MPO-positive cells in mice treated with DPH and BSO, DPH alone, or vehicle. Values represent the mean ± SEM of 4–5 specimens. The differences relative to the control mice (MPO-stained) or BSO-treated mice (ALT, AST, and T-Bil) were considered significant at $^{*}p < .05$, $^{**}p < .01$, and $^{***}p < .001$. Abbreviations: ALT, alanine aminotransferase; AST, aspartate aminotransferase; BSO, L-buthionine-S,R-sulfoximine; DPH, 5,5-diphenylhydantoin; T-Bil, total bilirubin.

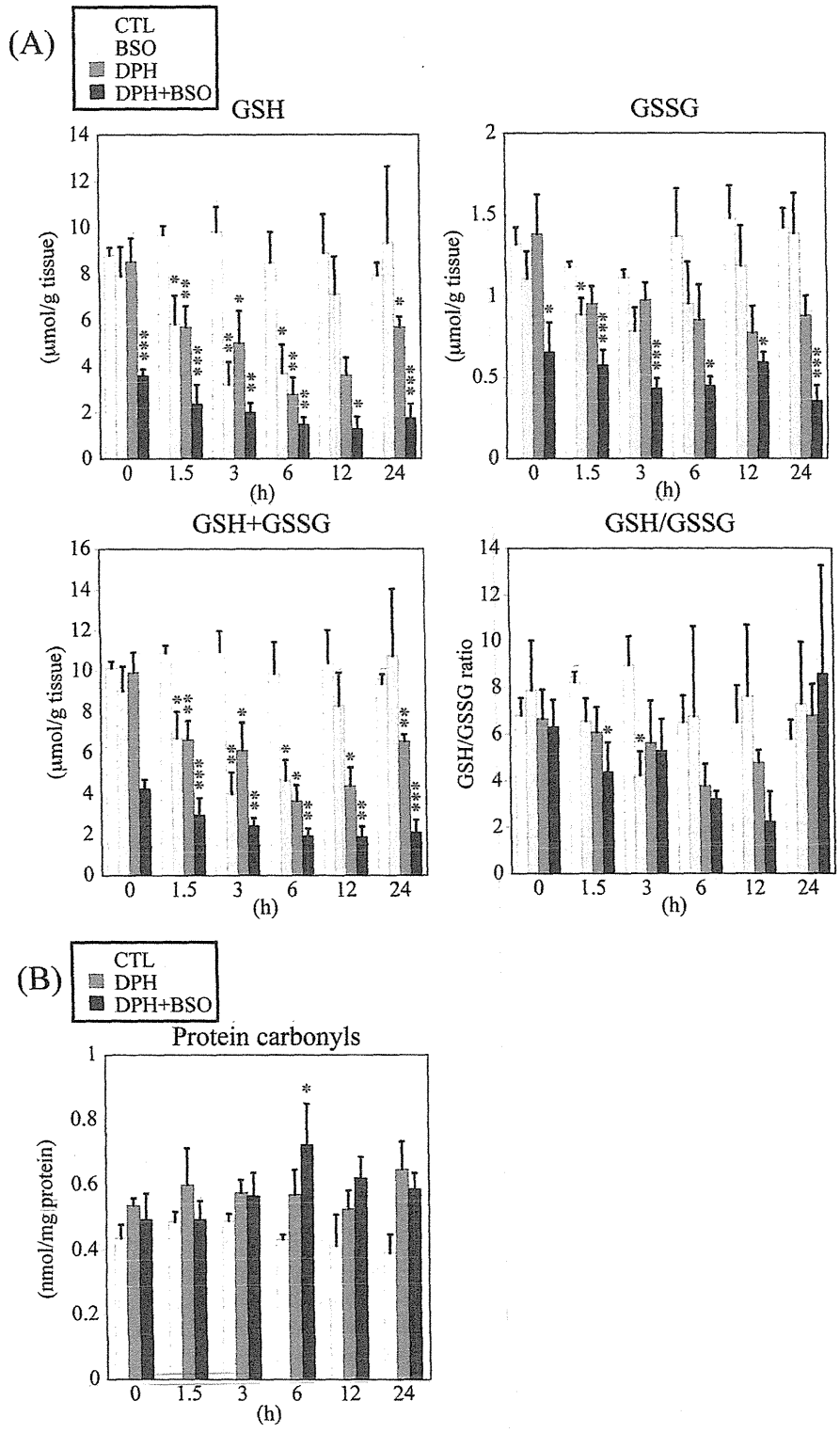

FIG. 2. Time-dependent changes in hepatic GSH, GSSG, and oxidative stress marker in DPH-induced liver injury. The mice were IP given DPH at 50 mg/kg for 2 days, and afterwards on days 3 through 5, DPH was orally administered at 100 mg/kg. BSO was IP injected 1 h prior to each DPH administration. Each vehicle was used as a control. At 0, 1.5, 3, 6, 12, and 24 h after the final DPH treatment, the liver was collected to measure the hepatic GSH, GSSG, and GSH + GSSG levels, the GSH/GSSG ratio (A), and the level of hepatic protein carbonyls (B). The data are shown as the mean ± SEM of the results from 4 to 5 mice. The differences relative to the control mice were considered significant at $*p < .05$, $**p < .01$, and $*** p < .001$. Abbreviations: DPH, 5,5-diphenylhydantoin; GSH, glutathione; GSSG, glutathione disulfide.

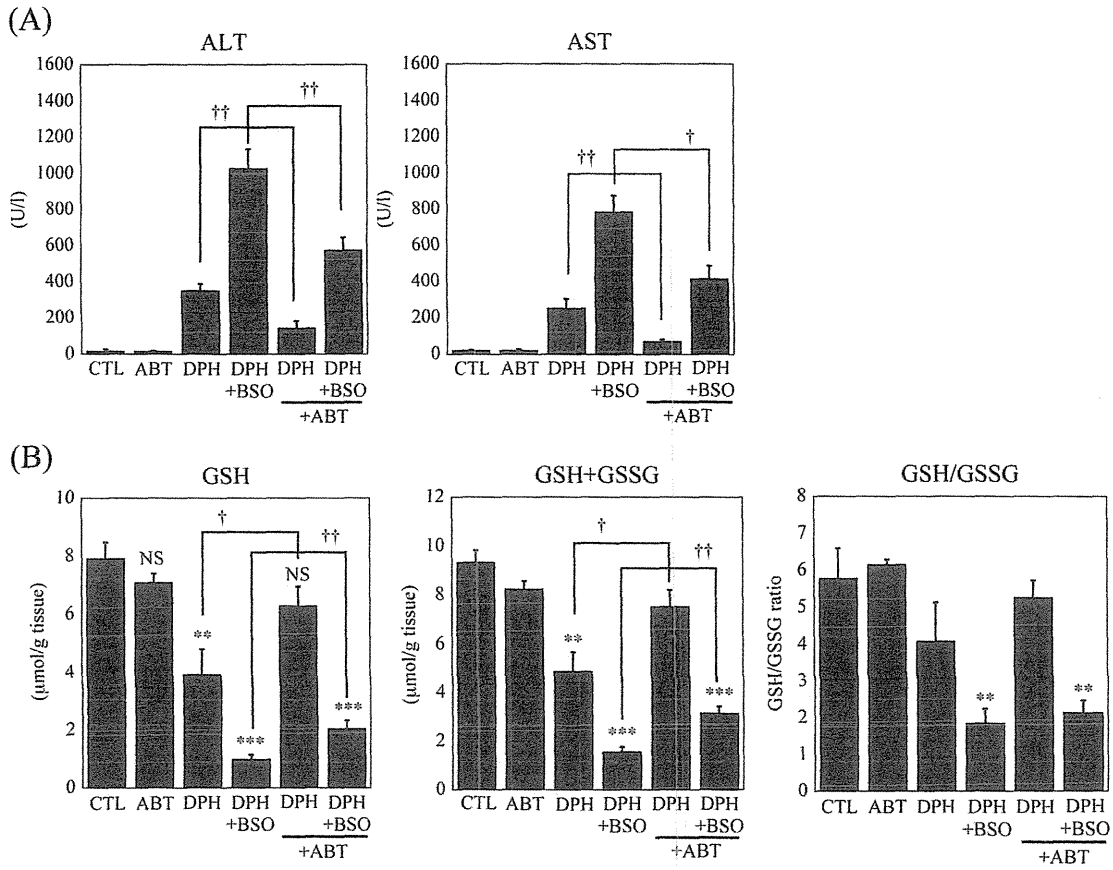

FIG. 3. Effect of a P450 inhibitor on plasma ALT and AST and hepatic GSH and GSSG levels in DPH-induced liver injury. The mice were IP given DPH at 50 mg/kg for 2 days, and then they were orally administered 100 mg/kg DPH on days 3 through 5. BSO was IP injected 1 h prior to each DPH treatment. ABT (100 mg/kg), a nonspecific inhibitor of P450, was IP given 1 h prior to the final DPH treatment. Each vehicle was used as a control. At 24 h after the final DPH treatment, the liver and plasma were collected to measure plasma ALT and AST levels (A), hepatic GSH and GSH + GSSG levels, and the GSH/GSSG ratio (B). The data are shown as the mean ± SEM of the results from 4 mice. The differences relative to the control mice were considered significant at $*p < .05$, $**p < .01$, and $*** p < .001$, and the differences between the ABT-treated and vehicle-treated mice were considered significant at $\dagger p < .05$, $\dagger\dagger p < .01$. Abbreviations: ABT, 1-aminobenzotriazole; ALT, alanine aminotransferase; AST, aspartate aminotransferase; DPH, 5,5-diphenylhydantoin; GSH, glutathione; GSSG, glutathione disulfide; NS, not significant.

at 1.5 h, and the expression level of S100A9 was significantly increased at 12 h after the final DPH treatment. To investigate whether HMGB1 is involved in the onset of inflammation, the plasma concentration of the HMGB1 protein was measured. HMGB1 is secreted from activated immune cells and is also released from necrotic cells. Therefore, we measured plasma HMGB1 protein levels using an ELISA and observed that they were significantly increased 3 h after the final DPH treatment in mice given both DPH and BSO (Fig. 4B). These results suggest that DAMPs are involved in the onset of inflammation.

To investigate whether TLR4 signaling and HMGB1 are involved in DPH-induced liver injury, eritoran, a specific TLR4 antagonist, or an anti-HMGB1 antibody was used. Treatment with either eritoran or the anti-HMGB1 antibody significantly suppressed the elevation of plasma ALT levels, suggesting that HMGB1 and TLR4 signaling may be involved in DPH-induced liver injury (Figs. 4C and D).

Changes in the Expression Levels of NALP3 Inflammasome-Related Factors

To investigate whether the NALP3 inflammasome is involved in the onset of inflammation, time-dependent changes in the hepatic mRNA expression levels of NALP3 and IL-1β were measured (Fig. 5A). The mRNA expression levels of IL-1β and NALP3 were significantly increased 1.5 h after the final DPH treatment. We then investigated whether the plasma concentration of the IL-1β protein is related to the onset of inflammation. The plasma IL-1β protein level was significantly increased 3 h after the final DPH treatment (Fig. 5B). These results suggest that NALP3 inflammasome activation leading to IL-1β production is involved in the onset of inflammation.

Changes in the Expression Levels of Th Cell-Related Transcription Factors, Cytokines, and Chemokines

To investigate whether inflammatory factors are involved in DPH-induced liver injury, we measured the time-dependent

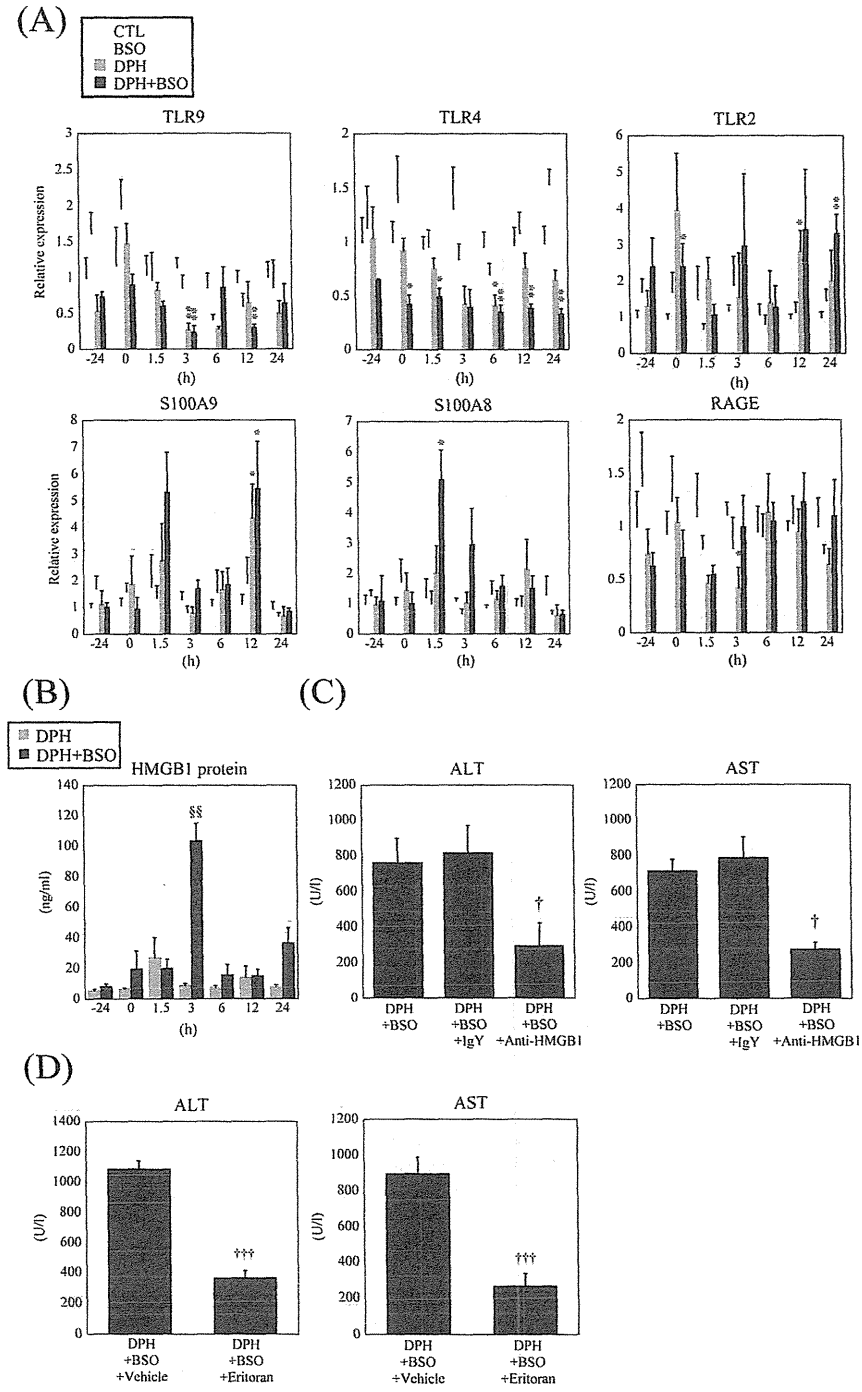

FIG. 4. Time-dependent changes in the hepatic mRNA expression levels of DAMP-related genes and plasma HMGB1 protein levels and the results of the neutralization studies in DPH-induced liver injury. A and B, Mice were IP given DPH at 50 mg/kg for 2 days, followed by oral administration of 100 mg/kg of DPH on days 3 through 5. BSO was IP injected 1 h prior to each DPH administration. Each vehicle was used as a control. At 24 h before (−24) and 0, 1.5, 3, 6, 12, and 24 h after the final DPH treatment, liver and plasma samples were collected to measure the expression of both the hepatic mRNAs of DAMP-related genes and the plasma HMGB1 protein. The expression levels of hepatic mRNAs were normalized to that of Gapdh. C, The effect of an anti-HMGB1 antibody. Mice were IV administered the anti-mouse HMGB1 antibody (200 μg anti-HMGB1 antibody in 0.2 ml sterile PBS) simultaneously with the final DPH treatment. Blood was collected 24 h after the final DPH treatment. D, The effect of eritoran, a TLR4 antagonist, on DPH-induced liver injury. Mice were IV given eritoran (50 μg/mouse in 0.2 ml sterile saline) simultaneously with the final DPH treatment. Blood was collected 24 h after the final DPH treatment. The data are shown as the mean ± SEM. The results of the time-dependent study are taken from 3 to 5 mice, and the other data are taken from 4 to 5 mice. The differences relative to the control mice were considered significant at $*p < .05$, $**p < .01$, compared with the −24 h mice were considered significant at §§$p < .01$ in ELISA, and compared with isotype IgY or vehicle-treated mice were considered significant at †$p < .05$ and †††$p < .001$ in neutralization or antagonist studies, respectively. Abbreviations: BSO, L-buthionine-S,R-sulfoximine; DAMP, damage-associated molecular patterns; DPH, 5,5-diphenylhydantoin; HMGB1, high-mobility group box 1; mRNA, messenger RNA; RAGE, receptor for advanced glycation end products; TLR, toll-like receptor.

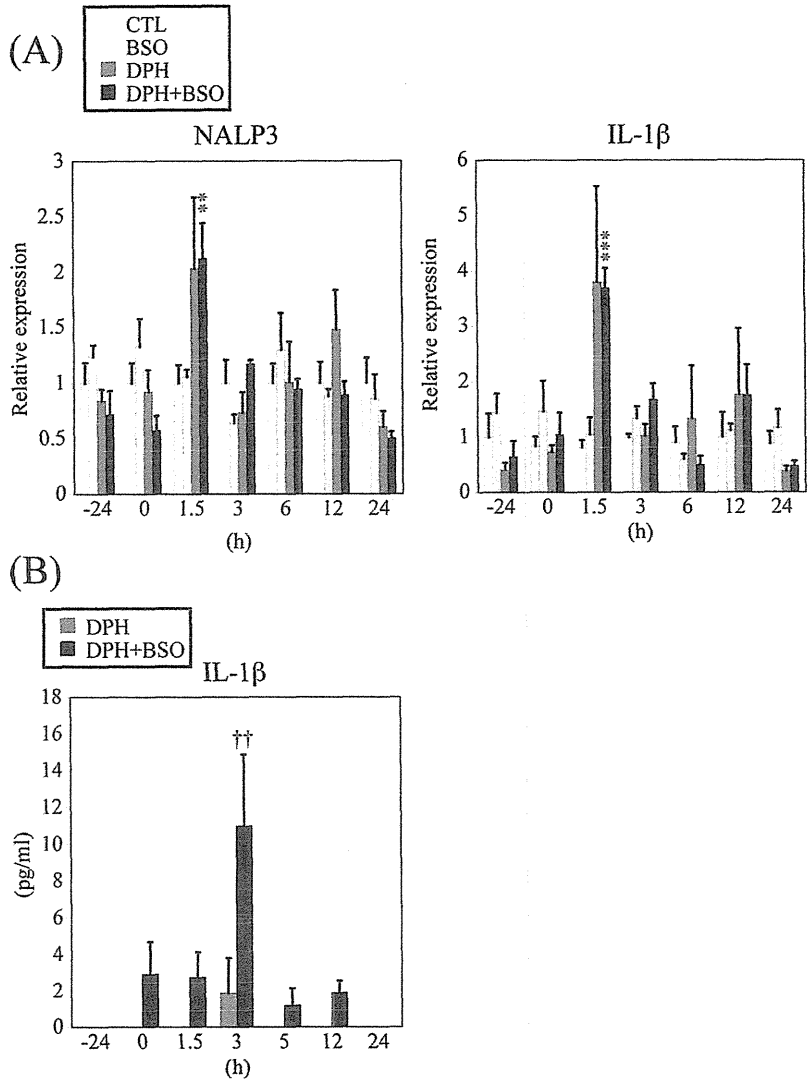

FIG. 5. Time-dependent changes in the hepatic mRNA expression levels of NALP3 and IL-1β (A) and plasma IL-1β protein levels (B) in DPH-induced liver injury. The experimental conditions for DPH treatments and blood and liver collection were the same as those in Figure 4. The data are shown as the mean ± SEM of the results from 3 to 5 mice. The differences relative to the control mice were considered significant at $^{**}p < 0.01$ and $^{***}p < 0.001$, and the -24 h mice were considered significant at $^{\dagger\dagger}p < 0.01$ in ELISA. Abbreviations: DPH, 5,5-diphenylhydantoin; IL, interleukin; NALP3, NACHT-, LRR-, and pyrin domain-containing protein 3; mRNA, messenger RNA.

changes in the hepatic mRNA expression levels of transcription factors for the Th lineage, cytokines, and chemokines (Fig. 6A). The hepatic mRNA expression levels of the Th17 cell-related factors IL-23 p19, IL-6, and ROR-γt were significantly increased at some time points of measurement in mice treated with both DPH and BSO compared with the vehicle-treated mice. However, the expression levels of T-bet, GATA-3, and Foxp3, corresponding to Th1-, Th2-, and regulatory T cell-related factors, respectively, were significantly decreased in mice treated with both DPH and BSO compared with vehicle-treated mice. Following the last administration of DPH in DPH plus BSO-treated mice, the expression levels of chemokines such as MCP-1 and MIP-2 showed a time-dependent increase. The expression levels of MIP-2 were significantly increased at 6–24 h after the last DPH administration in DPH plus BSO-treated mice compared with vehicle-treated mice. However, their levels in the mice given only BSO were not significantly altered compared with those in the mice given the vehicle. These results suggest that Th17 cell-mediated inflammation is involved in DPH-induced liver injury.

We next measured the plasma concentration of the IL-17 protein using an ELISA. A significant increase in concentration was observed at 6 h after the final DPH treatment in the mice given both DPH and BSO, whereas no significant increase was observed in the mice given only DPH (Fig. 6B). To investigate whether IL-17 was involved in DPH-induced liver injury, we

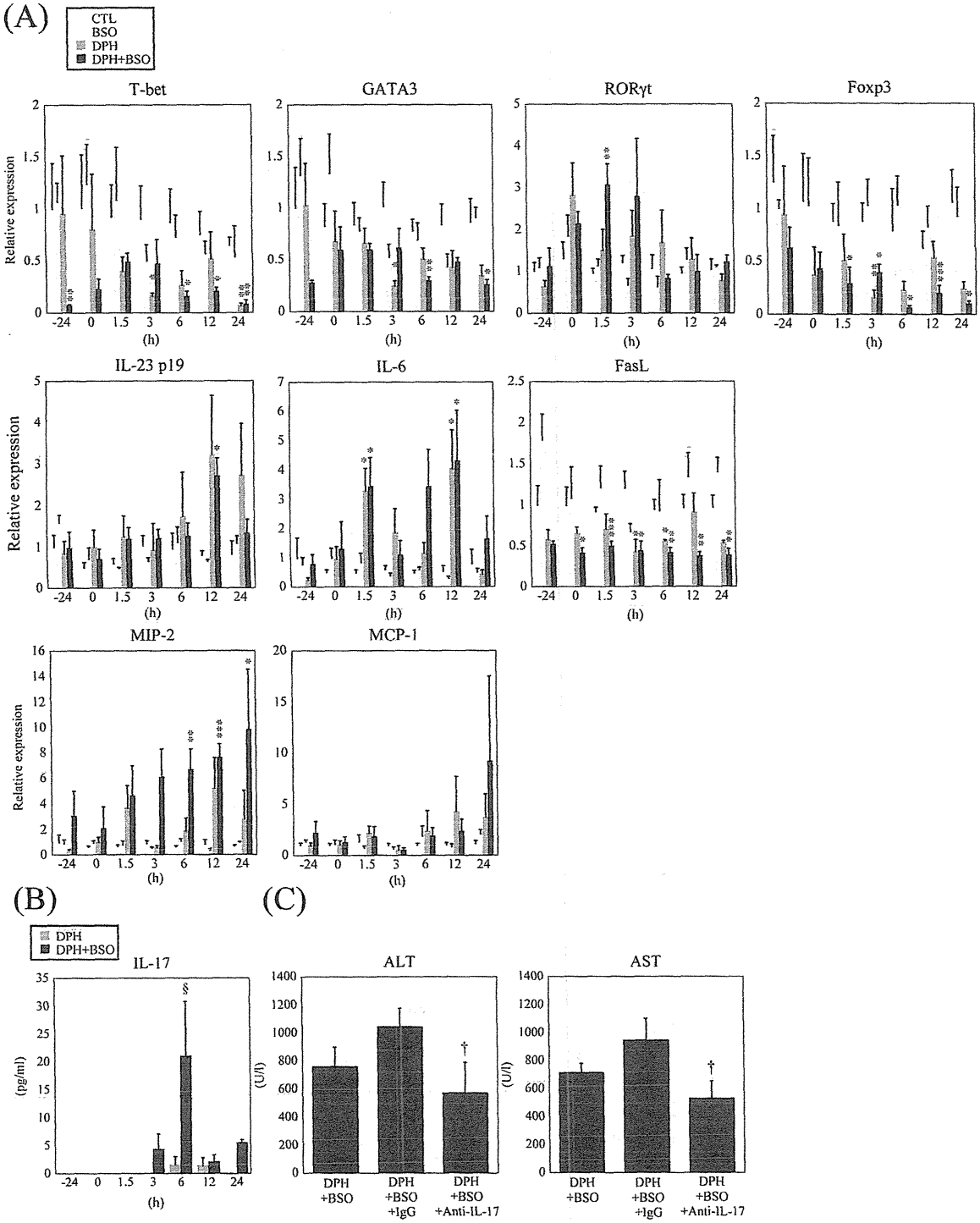

FIG. 6. Time-dependent changes in the hepatic mRNA expression levels and plasma protein levels and a neutralization study of proinflammatory cytokines and chemokines in DPH-induced liver injury. A and B, The experimental conditions for DPH treatments and blood and liver collection were the same as those in Figure 4. C, For the neutralization study, mice were IV injected with an anti-mouse IL-17 antibody (100 μg anti-mouse IL-17 antibody in 0.2 ml of sterile PBS) 3 h after the final DPH treatment. As a control, the IgG isotype was used. At 24 h after the final DPH treatment, plasma was collected to measure its ALT and AST levels. The data are shown as the mean ± SEM. The results of the time-dependent study are taken from 3 to 5 mice, and the results from the neutralization study are taken from 4 to 5 mice. The differences relative to the control mice were considered significant at $*p < .05$, $**p < .01$, and $***p < .001$; –24 h mice were considered significant §$p < .05$ in ELISA; and those compared with isotype IgG-treated mice were considered significant at †$p < .05$ in neutralization study. Abbreviations: ALT, alanine aminotransferase; AST, aspartate aminotransferase; DPH, 5,5-diphenylhydantoin; IL, interleukin; mRNA, messenger RNA.

performed a neutralization study. A monoclonal anti-mouse IL-17 antibody was IV injected 3 h after the final DPH treatment. As a result, the plasma ALT and AST levels were significantly decreased 24 h after the final DPH treatment compared with the levels in mice given an isotype IgG control antibody (Fig. 6C).

The Effect of Prostaglandin E_1 on Liver Injury

PGEs are known to protect against drug-induced and immune-mediated liver injury by downregulating the production of inflammatory cytokines. To investigate the therapeutic effect of PGE_1 on DPH-induced liver injury, PGE_1 conjugated with α-cyclodextrin was IP administered to mice 3 h after the final DPH treatment according to the previously reported method (Higuchi *et al.*, 2012; Kobayashi *et al.*, 2009). The plasma ALT and AST levels were significantly decreased in mice treated with both DPH and BSO compared with the vehicle-treated mice (Fig. 7A). In addition, 24 h after the final DPH treatment (Fig. 7B), PGE_1 treatment significantly decreased the hepatic MIP-2 mRNA levels, whereas the MCP-1 mRNA levels showed a tendency to decrease compared with the vehicle-treated mice. The mRNA expression levels of IL-6 and IL-23 p19 were not significantly changed by PGE_1 (data not shown) because these mRNA expressions were not changed 24 h after the final DPH treatment. In the histopathological evaluation study, PGE_1 treatment significantly decreased the number of MPO-positive cells (Figs. 7C and D). These results suggest that PGE_1 inhibits neutrophil infiltration, likely due to the suppression of Th17 cell function.

DISCUSSION

Development of an understanding of the mechanism of drug-induced liver injury has been hampered by the lack of a suitable animal model. In this study, we first developed a model for DPH-induced liver injury in mice. In particular, we examined different conditions such as the dose of DPH, the number of doses, the dosing method, and the addition of BSO. We succeeded in developing the mouse model for DPH-induced liver injury by administering DPH at 50 mg/kg (IP, approximately one-sixth of the IP LD_{50}) DPH plus BSO for 2 days followed by a dose of 100 mg/kg (p.o., approximately one-seventh of the oral LD_{50}) plus BSO for 3 days. The mice given this treatment showed marked hepatotoxicity (Figs. 1A and D).

DPH is metabolized into an arene oxide and a catechol metabolite in human liver microsomes, suggesting that reactive metabolites are likely implicated in hepatotoxicity (Munns *et al.*, 1997). There are a number of reports showing that BSO, when given together with a drug that causes liver injury in humans, will also cause drug-induced liver injury mouse and rat models (Shimizu et al., 2009, 2011) because GSH is the major antioxidant agent and is protective against toxicity by reactive metabolites or ROS. BSO is a specific inhibitor of γ-glutamylcysteine synthetase, a rate-limiting enzyme involved in GSH synthesis, and it can decrease GSH levels *in vivo* and *in vitro* (Watanabe *et al.*, 2003). In addition, BSO was shown to have no effect on the expression levels of microsomal CYPs and phase II conjugating enzymes such as glutathione-*S*-transferase (GST), sulfotransferase, and uridine diphosphate-glucuronosyltransferase (Drew and Miners, 1984; Griffith and Meister, 1979; Watanabe *et al.*, 2003). Therefore, we adapted a BSO combination method to deplete hepatic GSH. In this study, BSO was administered at a dose of 700 mg/kg 1 h prior to DPH treatment as described in previous studies (Shimizu et al., 2009, 2011). DPH treatment resulted in only a weak hepatotoxicity characterized by the elevation of plasma ALT levels, suggesting that GSH depletion likely exacerbates DPH-induced hepatotoxicity (Fig. 1A). These results indicate that GSH depletion is one of the risk factors for DPH-induced liver injury.

It has been reported that ROS generation is involved in drug-induced hepatotoxicity as reported in nimesulide (Ong *et al.*, 2006). Nimesulide causes mitochondrial impairment, as reflected by the decreasing mitochondrial ATP content and cytochrome C release. Therefore, we think that direct mitochondrial impairment, which is protected against by GSH, is partly involved in DPH-induced liver injury. In the histopathological analysis, apoptotic cells were observed, which might be partly caused by mitochondrial impairment (Fig. 1D).

P450 inhibitors suppressed the covalent binding of a DPH intermediate, and inducers of P450 enhanced the covalent bonding in hepatic microsomes taken from A/J mice (Roy and Snodgrass, 1990). Furthermore, GSH may modulate DPH metabolism either by trapping a DPH-reactive intermediate and decreasing the protein binding or by protecting proteins from attack by electrophilic or free radical intermediates of DPH (Roy and Snodgrass, 1990). Together, these studies and our data indicate that CYP-mediated covalent binding to hepatic proteins may be one of the mechanisms causing DPH-induced liver injury.

Administration of DPH without BSO results in a weak hepatotoxicity compared with a co-treatment with BSO, possibly due to the detoxification of reactive metabolites by GSH under normal conditions (Fig. 1A). Indeed, the administration of DPH caused significant decreases in hepatic GSH levels (Fig. 2A). The decrease in hepatic GSH content was more persistent in the mice treated with DPH plus BSO than in those treated with DPH only, and it could be that sustained reduction in GSH levels is important for toxicity.

The single administration study, even in combination with BSO, resulted in no hepatotoxicity, suggesting that the repeated administration of DPH is necessary for DPH-induced liver injury (Fig. 1B). DPH induces CYP3A4 and CYP2C9 in humans (Chaudhry *et al.*, 2010; Fleishaker *et al.*, 1995) and Cyp3a11 and Cyp2c29 in mice (Hagemeyer *et al.*, 2010), and these CYPs are involved in DPH oxidative metabolism. Therefore, the activation of DPH-inducible Cyps likely precedes

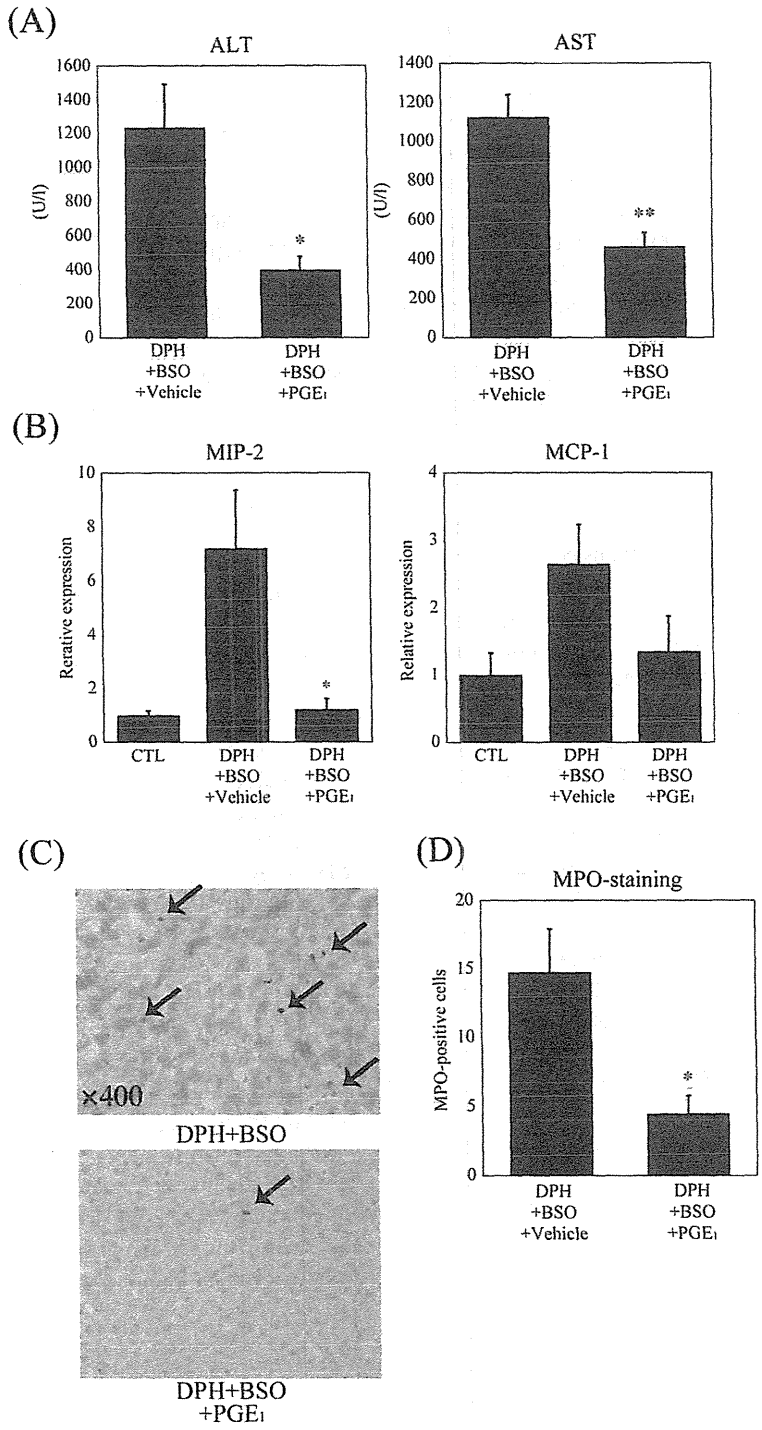

FIG. 7. Effects of PGE_1 on DPH-induced liver injury. The experimental conditions for DPH administration were the same as those in Figure 4. Mice were IP injected with PGE_1 (50 μg/mouse, dissolved in 0.5 ml sterile saline) 3 h after the final DPH treatment. Each vehicle was used as a control. At 24 h after the final DPH treatment, the plasma and liver were collected to measure the ALT and AST levels (A), the hepatic mRNA levels of MIP-2 and MCP-1 (B), and for immunohistochemistry (C and D). The expression level of hepatic mRNA was normalized to that of Gapdh. Mononuclear cell infiltration was assessed by immunostaining for MPO. The number of MPO-positive cells in DPH and BSO-treated or DPH, BSO, and PGE_1-treated mice is shown in (D). The arrows indicate MPO-positive cells. The data are shown as the mean ± SEM of the results from 4 to 5 mice. The differences compared with the DPH-treated, BSO-treated, and vehicle-treated mice were considered significant at $*p < .05$ and $**p < .01$. Abbreviations: ALT, alanine aminotransferase; AST, aspartate aminotransferase; BSO, L-buthionine-S,R-sulfoximine; DPH, 5,5-diphenylhydantoin; MCP-1, monocyte chemoattractant protein-1; MIP-2, macrophage inflammatory protein-2; MPO, myeloperoxidase; mRNA, messenger RNA; PGE_1, Prostaglandin E_1.

the onset of DPH-induced liver injury. During repeated dosing with DPH, even with BSO, no increase in ALT levels was observed on days 1–3 (Fig. 1A). We speculate that the quantity of DPH-inducible Cyps on the fourth day is sufficient to produce the reactive metabolites required for the development of liver injury. Pretreatment with ABT, a nonspecific inhibitor of P450 that can reduce the oxidative metabolism of drugs *in vivo* without any overt toxicity (Shimizu *et al.*, 2009), on the fifth day significantly suppressed the elevation of the ALT levels and the hepatic GSH depletion by DPH plus BSO (Fig. 3A). These data also indicate that P450-mediated metabolism is involved in DPH-induced liver injury.

Previous studies on DPH-induced liver injury in humans show severe hepatocellular injury with a prominent inflammatory response and massive necrosis (Mullick and Ishak, 1980). In this study, hepatic apoptosis, ballooning cells, and neutrophil infiltration were observed in DPH-induced liver injury in mice (Fig. 1D). Necrotic or apoptotic cells trigger a release of cell contents, and as a result, some of the released endogenous compounds are able to activate innate immune cells (Scaffidi *et al.*, 2002). HMGB1 is one of the first DAMPs identified, which is released during endogenous tissue trauma. However, a large number of other molecules, including heat shock proteins, S100A8/9, DNA, RNA, and others, can also function as DAMPs (Bianchi, 2007). The activation of innate immune cells by DAMPs occurs through TLRs, which recognize various molecular patterns including one in HMGB1 (Schwabe *et al.*, 2006).

Mature IL-1β protein is produced by cleavage of precursor IL-1β by caspase-1. The release of active IL-1β engages cells containing IL-1R and promotes inflammatory responses (Bryant and Fitzgerald, 2009; Latz, 2010). Therefore, we thought that IL-1β protein levels do not reflect the mRNA expression levels of IL-1β. Indeed, the mRNA levels of IL-1β were similar between DPH plus BSO-treated and DPH-treated mice, whereas the plasma IL-1β protein levels were significantly increased in DPH plus BSO-treated mice. As reviewed in Latz (2010), Schroder and Tschopp (2010), and Scaffidi *et al.*, 2002), the NALP3 inflammasome is activated by DAMPs that are released from injured cells. The NALP3 inflammasome generates mature IL-1β via proteolytic pathways. Recently, oxidative stress has been shown to play an important role in the activation of the NALP3 inflammasome (Bryant and Fitzgerald, 2009; Martinon *et al.*, 2009; Zhou *et al.*, 2010). In this study, DPH and BSO together significantly increased an oxidative stress marker, the protein carbonyl, suggesting that DPH-generated oxidative stress may be involved in the activation of the NALP3 inflammasome (Fig. 2B).

On the basis of our results, we speculate that the secretion of DAMPs from cells that are injured by reactive metabolites or ROS results in the activation of the NALP3 inflammasome and TLR4 signaling; these processes are factors in the early onset of liver injury because their mRNA levels were increased at relatively early time points. Additionally, we showed that HMGB1 and TLR4 are involved in DPH-induced liver injury (Figs. 4B and C).

Although the mechanism of drug-induced liver injury is still unclear due to the lack of animal models, LPS (lipopolysaccharide)-treated rodent models showed high sensitivity to human hepatotoxic drugs, such as trovafloxacin (Shaw *et al.*, 2009). LPS can activate innate immune responses via TLR4, which might suggest that the susceptibility to innate immune responses is one of the risk factors of DPH-induced liver injury.

In an adaptive immune reaction, Th17 cells may be involved in some types of drug-induced liver injury (Higuchi *et al.*, 2012; Kobayashi *et al.*, 2009). IL-1β and IL-6 or IL-1β together with IL-23 induce Th17 cell differentiation (Acosta-Rodriguez *et al.*, 2007). IL-17, which is produced mainly by a specific subset of Th17 cells, stimulates the production of CXC chemokines such as MIP-2 and plays an important role in neutrophil activity (Langrish *et al.*, 2005; Steinman, 2007). IL-17 is involved in autoimmune responses and some immune-mediated drug-induced liver injuries in mice (Higuchi *et al.*, 2012; Kobayashi *et al.*, 2009). These findings prompted us to investigate the involvement of IL-17 in DPH-induced liver injury. The neutralization of IL-17 significantly inhibited the previously increased plasma ALT and AST levels, suggesting that IL-17 is involved in DPH-induced liver injury (Fig. 6B).

A previous study showed that PGE_1 inhibited neutrophil superoxide production (Talpain *et al.*, 1995) and had a protective effect against drug-induced liver injury in mice. For mice with halothane- and carbamazepine-induced liver injuries, PGE_1 inhibits the increased plasma ALT and IL-17 levels, as well as the expression levels of hepatic MIP-2, IL-6, and IL-23 p19, suggesting that PGE_1 has a protective effect on IL-17-mediated liver injury (Higuchi *et al.*, 2012; Kobayashi *et al.*, 2009). In this study, the elevation of plasma ALT and AST levels, hepatic MIP-2 mRNA expression levels, and the number of hepatic MPO-positive cells were significantly inhibited by PGE_1 (Figs. 7A–C). As a result, we conclude that PGE_1 may be used for pharmacotherapy in DPH-induced liver injury.

In conclusion, in this study, we first established DPH-induced liver injury in mice. We demonstrated that DPH-induced liver injury is related to hepatic GSH levels, oxidative metabolism by Cyps, the innate immune response, and Th17 cell-mediated inflammation. These observations may aid in understanding the risk factors for and the mechanism of the idiosyncratic hepatotoxicity of DPH in humans.

FUNDING

Health and Labor Sciences Research Grants from the Ministry of Health, Labor and Welfare of Japan (H24-BIO-G001).

REFERENCES

Acosta-Rodriguez, E. V., Napolitani, G., Lanzavecchia, A., and Sallusto, F. (2007). Interleukins 1beta and 6 but not transforming growth factor-beta are essential for the differentiation of interleukin 17-producing human T helper cells. *Nat. Immunol.* **8**, 942–949.